RESEARCH ARTICLE

Global terrestrial nitrogen uptake and nitrogen use efficiency

Yunke Peng[1,2] | Iain Colin Prentice[3,4,5] | Keith J. Bloomfield[3] | Matteo Campioli[6] | Zhiwen Guo[7] | Yuanfeng Sun[8] | Di Tian[1,2,9] | Xiangping Wang[7] | Sara Vicca[6] | Benjamin D. Stocker[1,2,10,11]

[1]Department of Environmental Systems Science, ETH, Universitätsstrasse 2, Zurich, Switzerland; [2]Swiss Federal Institute for Forest, Snow and Landscape Research WSL, Birmensdorf, Switzerland; [3]Department of Life Sciences, Georgina Mace Centre for the Living Planet, Imperial College London, Ascot, UK; [4]Department of Biological Sciences, Macquarie University, North Ryde, New South Wales, Australia; [5]Department of Earth System Science, Tsinghua University, Beijing, China; [6]Research Group PLECO (Plants and Ecosystems), Department of Biology, University of Antwerp, Wilrijk, Belgium; [7]School of Ecology and Nature Conservation, Taiyueshan Long-Term Forest Ecosystem Research Station, Beijing Forestry University, Beijing, China; [8]Institute of Ecology, College of Urban and Environmental Sciences, and Key Laboratory for Earth Surface Processes of the Ministry of Education, Peking University, Beijing, China; [9]The Key Laboratory for Silviculture and Conservation of Ministry of Education, Beijing Forestry University, Beijing, China; [10]Institute of Geography, University of Bern, Bern, Switzerland and [11]Oeschger Centre for Climate Change Research, University of Bern, Bern, Switzerland

Correspondence
Yunke Peng
Email: yunke.peng@usys.ethz.ch

Abstract

1. Plant biomass production (BP), nitrogen uptake (N_{up}) and their ratio, and nitrogen use efficiency (NUE) must be quantified to understand how nitrogen (N) cycling constrains terrestrial carbon (C) uptake. But the controls of key plant processes determining N_{up} and NUE, including BP, C and N allocation, tissue C:N ratios and N resorption efficiency (NRE), remain poorly known.

2. We compiled measurements from 804 forest and grassland sites and derived regression models for each of these processes with growth temperature, vapour pressure deficit, stand age, soil C:N ratio, fAPAR (remotely sensed fraction of photosynthetically active radiation absorbed by green vegetation) and growing-season average daily incident photosynthetic photon flux density (gPPFD; effectively the seasonal concentration of light availability, which increases polewards) as predictors. An empirical model for leaf N was based on optimal photosynthetic capacity (a function of gPPFD and climate) and observed leaf mass per area. The models were used to produce global maps of N_{up} and NUE.

3. Global BP was estimated as 72 Pg C/year; N_{up} as 950 Tg N/year; and NUE as 76 g C/g N. Forest BP was found to increase with growth temperature and fAPAR and to decrease with stand age, soil C:N ratio and gPPFD. Forest NUE is controlled primarily by climate through its effect on C allocation—especially to leaves, being richer in N than other tissues. NUE is greater in colder climates, where N is less readily available, because below-ground allocation is increased. NUE is also greater in drier climates because leaf allocation is reduced. NRE is enhanced (further promoting NUE) in both cold and dry climates.

4. *Synthesis.* These findings can provide observationally based benchmarks for model representations of C–N cycle coupling. State-of-the-art vegetation models in the

TRENDY ensemble showed variable performance against these benchmarks, and models including coupled C–N cycling produced relatively poor simulations of N_{up} and NUE.

KEYWORDS

carbon, climate, data-driven model, global change ecology, nitrogen uptake, nitrogen use efficiency, stand age, terrestrial ecosystem

1 | INTRODUCTION

Although the main fluxes in the terrestrial carbon (C) cycle are relatively well quantified, large uncertainty surrounds many aspects of the nitrogen (N) cycle (Davies-Barnard et al., 2020; Le Quéré et al., 2018; Zaehle et al., 2014). The two are inextricably linked (Cleveland et al., 2013; Hungate et al., 2003) because of the N requirements for plant growth (Norby et al., 2010), with N availability influencing the relationships among photosynthesis and growth (LeBauer & Treseder, 2008; Liang et al., 2020; Vicca et al., 2012), biomass production (BP) and allocation (Fay et al., 2015; Poorter et al., 2012; Terrer et al., 2019), and rhizodeposition (Henneron et al., 2020; Perkowski et al., 2021). Yet, recent ecosystem models have reported global plant N uptake (N_{up}) ranging widely, from 465 to 1197 Tg N year^{-1} (Cleveland et al., 2013; Goll, Winkler, et al., 2017; Lawrence et al., 2019; Oleson et al., 2010; Smith et al., 2014; Wiltshire et al., 2021). Although N cycling processes are expected to constrain the response of terrestrial C uptake to rising CO_2 (Hungate et al., 2003), the assumptions about these processes made in current models vary considerably and global compilations of site-level C and N cycling remain underused for their evaluation (see, e.g. Zaehle et al., 2014; Fowler et al., 2015). As a consequence, process-based models make widely divergent predictions of the extent of N limitation to global C uptake in scenarios of future CO_2 and climate change (Arora et al., 2020; Stocker et al., 2016; Zaehle et al., 2014).

Meanwhile, observational studies have generated a substantial body of ecosystem-level observations relevant to N cycling that has not previously been used in model development or evaluation. Here, we use such data, derived from multiple sources, to fit and upscale statistical models of key processes contributing to the terrestrial N cycle, with a view to providing new benchmarks to test (and potentially, better constrain) process-based models.

The starting point for our analysis is BP, which is distinct from net primary production (NPP). NPP is defined as gross primary production (total photosynthetic carbon fixation) minus plant respiration, while BP is the annual C actually used for the growth of leaves (BP_{leaf}), wood (BP_{wood}) and roots (BP_{root}; Collalti et al., 2020; Collalti & Prentice, 2019; Vicca et al., 2012). NPP includes the production of nonstructural C compounds, including labile carbohydrates, volatile organic compounds (VOC) and root exudates (Collalti et al., 2020; Vicca et al., 2012) that do not form part of BP. However, although BP is readily available from field measurements (albeit with uncertainties—especially about the below-ground contribution, and the variable contribution of nonstructural carbohydrates to

measured BP), NPP generally is not. Our particular focus is then on N_{up} and on nitrogen use efficiency (NUE), which is the ratio of BP to N_{up}. To estimate N_{up} and NUE, we analyse the environmental dependencies of the various components contributing to determining N cycling rates, including BP, biomass allocation, tissue C:N ratios and N resorption efficiency (NRE).

BP has been found to increase with growth temperature (Baig et al., 2015) and soil nutrient availability (LeBauer & Treseder, 2008). A decline in forest BP with stand age is also well documented (Ryan et al., 2004; Xia et al., 2019). Few attempts have been made to describe global variations of N_{up} and NUE (but see Cleveland et al., 2013; Wang, Ciais, et al., 2018). NUE has been indicated to increase as N supply becomes more limiting (Finzi et al., 2007; Harrington et al., 2001), and to be reduced at increased soil nitrogen-to-phosphorus (N:P) ratios (Gill & Finzi, 2016) or after N fertilization (Davies-Barnard et al., 2020). Variations in biomass distribution between different organs and their distinct C:N stoichiometry (Ma et al., 2021; Tian et al., 2019; Zhang et al., 2020), and variations in NRE (Deng et al., 2018; Du et al., 2020), must influence NUE, but there is limited knowledge of how these factors change along environmental gradients and of their importance in affecting N_{up} and NUE variations among sites with different climatic and edaphic conditions. Leaf stoichiometry not only varies greatly between species (Tian et al., 2019) but also shows systematic relationships with climate (Reich et al., 2007) and soils (Maire et al., 2015). Variations in mass-based foliar N content (N_{mass}, mg g^{-1}) have been interpreted as reflecting plant nutritional status (e.g. Penuelas et al., 2020) but N_{mass} depends in part on leaf mass per unit area (LMA) and in part on the amount of N invested in Rubisco, the key enzyme determining photosynthetic capacity (Dong et al., 2017; Luo et al., 2021). Photosynthetic capacity can be quantified by the maximum rate of carboxylation (V_{cmax}). When standardized to 25°C (V_{cmax25}), this rate is related to the amount of Rubisco in leaves and therefore to the amount of N per unit leaf area (Harrison et al., 2009). A substantial proportion of V_{cmax25} variation can be predicted by climate (Peng et al., 2021; Smith et al., 2019) and the same is true for LMA (Dong, Prentice, et al., 2022; Wang et al., 2023), implying that foliar N content is at least partly controlled by climate. NRE has been shown to be negatively related to temperature and humidity. Because rates of N cycling are enhanced in warmer and wetter environments, N supply from resorption becomes relatively less important under these conditions: As temperature and humidity increase, N cycling rates shift from the (more conservative) resorption pathway to the mineralization pathway (Deng et al., 2018; Du et al., 2020). Taken together,

climate likely influences the vegetation demand for N and the efficiency with which the uptake of N is translated into plant growth.

BP has been simulated by using satellite products (Cleveland et al., 2013; Zhao & Running, 2010), or with models entirely driven by climate (Goll, Winkler, et al., 2017; Lienert & Joos, 2018; Mauritsen et al., 2019; Meiyappan et al., 2015). However, variations in C allocation with climate and soil nutrient availability, and their implication for N uptake, have typically been underestimated in models (Medlyn et al., 2015; Zaehle et al., 2014). As a step towards remedying this situation, we compiled a new global dataset of the key components determining N cycling rates in terrestrial ecosystems (BP, allocation, plant C:N stoichiometry and NRE) and associated environmental drivers and vegetation characteristics (climate, vegetation cover, stand age and soil C:N ratio) and analysed their interrelationships using statistical methods (Figure S1). We upscaled and combined the resulting statistical models to produce global maps of BP, N_{up} and NUE. We also made a first assessment of the ability of process-based terrestrial C and C–N cycle models from the TRENDY ensemble to represent the environmental responses of BP, N_{up} and NUE as shown in our analysis.

2 | METHODS

The analysis was conducted in six stages: (1) compilation of a dataset of previously published stand-scale measurements for forest and grassland sites; (2) fitting statistical models at the stand scale; (3) global application of the models, to estimate global terrestrial C and N uptake; (4) global compilation of data to be used as predictors in statistical models; (5) analysis of the factors contributing to modelled N_{up} and NUE; and (6) comparison of the fitted statistical models with simulations by state-of-the-art global vegetation models.

2.1 | Stand-scale datasets of plant- and leaf-trait data

Our plant-trait dataset comprises measurements of total BP ($gCm^{-2}year^{-1}$) and the BP of leaves, wood and roots in forest (Anderson-Teixeira et al., 2016, 2018; Campioli et al., 2015; Luyssaert et al., 2007; Malhi et al., 2011, 2017; Tian et al., 2019; Vicca et al., 2012; Wang & Zhao, 2022); and total BP, the BP of leaves and roots in grassland (see Table S1 for citations of 78 original papers). Eighty-seven per cent of the data are from forests, 13% from grasslands. Seventeen per cent, 62% and 21% of the data are from tropical (0–22.5°), temperate (22.5°–50°) and high-latitude (>50°) regions, respectively. BP_{leaf}, BP_{wood} and BP_{root} represent leaf, wood and root production, with BP_{wood} equal to zero in grasslands. BP_{root} includes both fine and coarse (lignified) roots for forests and fine roots only for grasslands. Subterranean stems and rhizomes of grasses are implicitly included in roots. Total above-ground BP (ABP) is the sum of BP_{leaf} and BP_{wood}. Below-ground BP (BBP) is equal to BP_{root}. For a subset of the sites, we also obtained data on leaf C:N ratios, which

were used to calculate the leaf N flux (BP_{leaf} divided by the leaf C:N ratio, $gNm^{-2}year^{-1}$).

We assembled an additional leaf-trait dataset including N_{area}, V_{cmax25} and leaf mass per area (LMA), comprising 350 sites and 2424 species in natural (unfertilized) vegetation (Atkin et al., 2015; Bahar et al., 2017; Bloomfield et al., 2019; Cernusak et al., 2011; Domingues et al., 2010, 2015; Dong et al., 2017; Maire et al., 2015; Meir et al., 2017; Walker et al., 2014; Wang, Harrison, et al., 2018; Xu et al., 2021). Nitrogen resorption efficiency (NRE) data were obtained from published sources at 210 sites (Deng et al., 2018; Du et al., 2020).

For comparison with N_{up}, we used a forest net mineralization rate (N_{min}, $gNm^{-2}year^{-1}$) dataset from 225 samples at 84 sites (Gill & Finzi, 2016). Net mineralization is the net microbial release of inorganic N into the soil after accounting for immobilization of mineral N by microbes and constitutes the flux of mineral N that potentially becomes available for plant uptake (before accounting for N losses through leaching and gaseous pathways). Field measurements of N_{min} may be affected by plants taking up a fraction of the gross N mineralization flux, potentially leading to an underestimation of plant N uptake when using N_{min} as a proxy. Additionally, N_{min} might underestimate N_{up}, as a significant contribution to N_{up} can be via organic forms of N (Liu et al., 2017; Näsholm et al., 2009). In contrast, comparing N_{up} with N_{min} rests on the assumption that annual ecosystem N gains and losses are small compared with mineralization and uptake and thus implies an overestimation of N uptake estimated by N_{min}. However, because direct measurements of N_{up} are not possible (and ecosystem N_{up} estimates are commonly derived from the same component fluxes and stoichiometry data that were used in our model development), N_{min} was considered here as an acceptable independent point of comparison for modelled N_{up} (Gill & Finzi, 2016).

2.2 | Empirical models

Statistical models for BP, the allocation of BP to separate tissues, tissue C:N ratios and NRE were developed based on data from globally distributed forest and grassland sites (Figure S2). We used interpolated (rather than directly measured) values to avoid the ~86% reduction of sample size that would have occurred otherwise. Additional analyses, to test the validity of this choice, were carried out using directly measured values only.

For forests, a dataset of measured BP ($n = 514$; Figure S2), ABP ($n = 709$), BP_{leaf} ($n = 637$) and site-level predictors interpolated from map products was used to fit statistical models. BP and its allocation have previously been modelled as functions of stand age (Campioli et al., 2015), soil fertility (Vicca et al., 2012) and climate (Collalti et al., 2020). Accordingly, we initially selected the following six variables for predicting BP, ABP/BP and BP_{leaf}/ABP in forest: stand age, soil C:N ratio, fAPAR, T_g, gPPFD and vapour pressure deficit (D). Soil C:N provides an inverse indicator of soil N availability (Vicca et al., 2018). fAPAR represents an inverse measure of environmental stress—for example, because of

a short growing season or to low light, water or nutrient availability. gPPFD is in effect a measure of the seasonal concentration of light availability and, unlike total growing-season PPFD, increases towards the poles. (The selection of predictors was nearly unchanged if total PPFD was used instead of gPPFD to predict BP, except that total PPFD was finally not selected, and D was newly included.) To obtain values of predictor (independent) variables for each site, we three-dimensionally (latitude, longitude and elevation) interpolated values from global maps (see Section 2.4) to site locations using geographically weighted regression (GWR) in the '*spgwr*' package in R to obtain plot-level predictors for empirical model fitting.

Model selection (Table S2) was performed by forward stepwise regression, adding the variable producing the largest increase in R^2 at each step. We required all variables included in the final model to have regression coefficients significantly different from zero (assessed by the *t*-statistic). Variables were added one-by-one until this criterion was no longer met. All ratios constituting response variables in the statistical models (ABP/BP, BP_{leaf}/ABP and NRE) were logit-transformed, because these ratios range from 0 to 1; thus, values after transformation are continuous and unbounded, consistent with the assumptions of ordinary linear regression. For the same reason, stand age, soil C:N ratio, gPPFD and D were log-transformed. In one case—logit (BP_{leaf}/ABP)—the model selection procedure failed, as age was identified as the first predictor but became nonsignificant as more variables were added. In this case, we repeated the model selection with stand age removed.

Because multiple individual trees might have been measured at each site, a mixed-effects model was applied with site as the grouping variable for random offsets. Variance inflation factors (VIF) were calculated to test for multicollinearity in the BP and allocation models (Figure S3). T_g and D were found to cause multicollinearity in BP and ABP/BP models (VIF > 10), so in these two models we included T_g but not D.

Following Dong et al. (2017), leaf N_{area} can be well approximated as the sum of a bulk leaf tissue component proportional to LMA, and a metabolic component proportional to V_{cmax25}:

$$N_{area} = n_s LMA + n_r V_{cmax25}, \qquad (1)$$

where n_s and n_r are empirical coefficients. It follows that:

$$N_{mass} = n_s + n_r \frac{V_{cmax25}}{LMA}. \qquad (2)$$

We fitted this N_{mass} model using parallel observations of N_{mass}, V_{cmax25} and LMA, for 350 global sites and 2424 species. Here, site and species were treated as grouping variables for random offsets using a linear mixed-effects model with a crossed random design. To estimate leaf C:N ratio (C_{mass}/N_{mass}), leaf C_{mass} was assumed globally constant at the median value ($0.47\,g\,g^{-1}$) of the relevant subset of our leaf-trait dataset ($n = 79$ sites, 2492 individuals). This is consistent with recently reported global values of C_{mass} (Ma et al., 2018; Tang et al., 2018). Wood C:N ratio was assigned a value of $319\,g\,g^{-1}$, the global mean value of trunk C:N

ratio ($n = 544$ individuals) reported by Zhang et al. (2020). Root C:N ratio was assigned a value of $94\,g\,g^{-1}$ ($n = 22$ sites), which was derived here as the median value of measurements taken along with BBP measurements in our dataset. Although variations in wood and root C:N ratios are not negligible (Schreeg et al., 2014; Zhang et al., 2019), we treated them as constants here. Their variation appears to be more strongly controlled by phylogeny than by the environment (Zhang et al., 2020), rendering them less suitable for global upscaling with environmental covariates.

Following the finding by Deng et al. (2018) that NRE decreases with temperature and humidity, we fitted a linear model for NRE as a function of T_g and D at 184 forest sites (Deng et al., 2018; Du et al., 2020):

$$\text{logit (NRE)} = N_1 T_g + N_2 \ln D. \qquad (3)$$

For grasslands, model selection showed that the optimal predictive model for site-mean BP ($n = 119$ sites) was fitted by T_g and gPPFD, consistent with the model fitted for forest biomes. ABP/BP ($n = 109$ sites) was nonsensitive or weakly correlated to climate predictors. Therefore, we estimated a constant value for this ratio by performing a linear regression without intercept of ABP on BP, yielding a value of 0.50. Tissue C:N ratio and NRE data for grasslands had small sample sizes, rendering fitted models insufficiently robust. Therefore, leaf and root C:N ratios were assigned constant values of 18 and 41, respectively, and NRE = 69%, all being median values across the data for grasslands.

Total N uptake (N_{up}; $g\,N\,m^{-2}\,year^{-1}$) was estimated as:

$$N_{up} = N_{leaf} (1 - NRE) + N_{wood} + N_{root}, \qquad (4)$$

where N_{leaf} is BP_{leaf} divided by the leaf C:N ratio, N_{wood} (in forests) is BP_{wood} divided by the wood C:N ratio, and N_{root} is BP_{root} divided by the root C:N ratio. No resorption of N stored in roots was considered.

2.3 | Global mapping

The empirical models, developed based on site-specific observations, were applied globally—driven by global gridded data (see Section 2.4)—to obtain upscaled estimates of all component fluxes. Global maps were initially created for forests and grasslands separately (see Equations 1–4). The MODIS IGBP land-cover map (Sulla-Menashe & Friedl, 2018) was then used to determine the fraction of forests versus grasslands in each grid cell. Six land-cover classes (evergreen needleleaf, evergreen broadleaf, deciduous needleleaf, deciduous broadleaf, mixed forests and shrublands) were treated as forest, and one as grassland. The final value assigned to each grid cell was a weighted average of the values for forests and grasslands; weighting was based on the relative cover of forests versus grasslands, normalized to a sum of 100% (thus disregarding, e.g. urban or agricultural land in order to focus on natural and seminatural vegetation). The uncertainties of global estimations of C and N uptake were computed using standard error propagation methods. Negative BP values arising in a few

cases (0.2% and 1.4% of global grid cells in forest and grassland, respectively) were ignored. Global NUE was calculated based on area-weighted BP and N_{up} in each grid cell.

2.4 | Global datasets of predictors

For globally upscaling fluxes based on empirical models, we compiled global gridded datasets for all predictor (independent) variables used in the models. Maps on a half-degree global grid were developed for V_{cmax25} (μmol m^{-2} s^{-1}), mean daytime air temperature (T_g, °C), vapour pressure deficit (D, kPa), incident photosynthetic photon flux density averaged over the growing season (gPPFD, μmol m^{-2} s^{-1}), the fraction of absorbed photosynthetically active radiation (fAPAR, unitless: a remotely sensed measure of green vegetation cover), stand age (years), soil C:N ratio (g g^{-1}) and leaf mass per area (LMA, g m^{-2}; Figure S4).

The global map of V_{cmax25} was obtained using a climatically driven model for V_{cmax}, based on eco-evolutionary optimality principles (Peng et al., 2021; Prentice et al., 2014; Stocker et al., 2020; Wang et al., 2017). Global patterns of V_{cmax} predicted by this model have been shown to compare well to independent estimates derived from remotely sensed chlorophyll measurements (Dong, Wright, et al., 2022). V_{cmax} was predicted using Equation C4 in Stocker et al. (2020), from atmospheric pressure, CO_2, gPPFD and other daily climate forcing data (relative humidity, precipitation and average daily temperature) derived from WATCH Forcing Data ERA-Interim (WFDEI: Weedon et al., 2014). Values were converted to a standard temperature of 25°C (V_{cmax25}) using the Arrhenius equation, with activation energy from Bernacchi et al. (2001). This converts V_{cmax} predicted by the model, which applies to growth temperature and therefore reflects optimality under natural field conditions, to a quantity (V_{cmax25}) assumed proportional to Rubisco amount—and thus to the metabolic component of leaf N (Dong et al., 2017; Dong, Prentice, et al., 2022). Estimated V_{cmax25} was averaged over 1982–2011, using the maximum daily V_{cmax25} value for each year.

Monthly average values of mean daily maximum (T_{max}, °C) and minimum (T_{min}, °C) temperature were obtained from Climate Research Unit data (CRU TS 4.0; Harris et al., 2014) for the period 1980–2016. T_g was estimated monthly by approximating the diel temperature cycle with a sine curve, where daylight hours are determined by month and latitude:

$$T_g = T_{max}\left\{1/2 + \left(1 - x^2\right)^{1/2}/2\cos^{-1}x\right\} \\ + T_{min}\left\{1/2 - \left(1 - x^2\right)^{1/2}/2\cos^{-1}x\right\}, x = -\tan\lambda\tan\delta, \quad (5)$$

where λ is latitude and δ is the monthly average solar declination (Jones, 2013). Monthly values of T_g were averaged from 1980 to 2016, over the thermal growing season, that is, months with $T_g > 0$°C.

Vapour pressure deficit (D) was estimated using gridded actual vapour pressure (e_a, hPa) from CRU, for the same period and resolution as T_g, using GWR:

$$D = e_s - 0.1\,e_a, \text{where } e_s = 0.611\exp\left[17.27\,T_g / \left(T_g + 237.3\right)\right]. \quad (6)$$

Monthly values of D were averaged from 1980 to 2016 over the thermal growing season.

Incident solar radiation data were obtained from WFDEI for the same period and resolution as D and T_g. Solar radiation (W m^{-2}) was converted to gPPFD assuming an energy-flux ratio of 4.6 μmol J^{-1} and a photosynthetically active fraction of 0.5. Monthly values were averaged from 1980 to 2016 over the thermal growing season.

Fraction of absorbed photosynthetic radiation (fAPAR) data were derived from Advanced Very High Resolution Radiometer (AVHRR) Normalized Difference Vegetation Index third generation (NDVI3g) map products for the period 1982–2011 (Pinzon & Tucker, 2014). Mean stand age was derived from Poulter et al. (2018), calculated as the mean age across four plant functional types (PFTs) and 15 age classes (from 0–10 to 140–150 years), weighted by their respective fractional area coverage within each grid cell. Missing values for stand ages were filled by the average of the local continent. Soil C:N ratio (Batjes, 2015) was processed by calculating the layer depth-weighted mean across the top 2–3 layers (20–60 cm). Global soil C:N maps were then aggregated from 1/120 to 1/2 degrees and spatially interpolated to fill the 8% of land area with missing C:N values based on the k-nearest-neighbour (KNN) method, using longitude and latitude as predictors and an optimized $k = 7$. LMA (Moreno-Martínez et al., 2018) was also gap-filled by the KNN method (as predicted by latitude, T_g, gPPFD and the ratio of actual evapotranspiration to potential evapotranspiration, optimal $k = 9$), filling 71% of the land area.

2.5 | Factors contributing to NUE and N_{up}

We conducted a variable importance analysis using the Lindeman, Merenda and Gold (LMG) statistic (Grömping, 2006) for N_{up} and NUE separately in relation to all predictor variables, based on the global gridded data. LMG statistics were calculated only for the forest models because N cycling rates in grassland depended only on T_g and gPPFD and showed little variation.

2.6 | Comparison with global vegetation models

We analysed global simulations, by 12 dynamic global vegetation models (DGVMs) in version 8 of the TRENDY model ensemble, driven by varying CO_2 and climate but with fixed (preindustrial) land use (the S2 simulation protocol). The same simulations also contributed to the annual Global Carbon Budget publication for 2019 (Friedlingstein et al., 2019). The models do not distinguish BP from NPP, so we compared our BP values with DGVM-simulated NPP (variable 'NPP' in TRENDY outputs). We also compared our N_{up} values with DGVM-simulated N_{up} (variable 'fN$_{up}$' in TRENDY outputs). These comparisons were made using values extracted from global simulations for the same sites as in other analyses.

Because all the TRENDY DGVMs and our statistical models used climate variables as predictors, we also compared partial residual

relationships based on linear regressions for predicted site-level BP, N_{up} and NUE in relation to T_g, gPPFD and D.

3 | RESULTS

3.1 | Predicting component fluxes

Component fluxes showed stronger environmental dependencies, and more accurate predictions, in forests than in grasslands.

In forests (Table 1; Figure 1), BP and ABP/BP both decreased with increasing gPPFD (growing-season mean PPFD), soil C:N ratio and stand age but increased with growth temperature. (Note that gPPFD tends to be greater if the growing season is shorter, thus decreasing BP.) BP also increased with fAPAR. This result is expected because photosynthesis depends on canopy

TABLE 1 Empirical models and constants.

Response variables	Fitted regressions	R^2
Forest		
BP	$2838 + 15.7\,T_g - 278 \ln \text{gPPFD} - 377 \ln$ C:N $- 91.1 \ln$ age $+ 861$ fAPAR	0.44
logit ABP/BP	$14.9 + 0.0249\,T_g - 1.74 \ln \text{gPPFD} - 1.44 \ln$ C:N $- 0.134 \ln$ age	0.17
logit BP_{leaf}/ABP	$-12.0 + 1.82 \ln \text{gPPFD} + 1.02$ fAPAR $- 0.485 \ln D$	0.08
Leaf N_{mass}	$0.00584\,V_{cmax25}$/LMA $+ 0.0161$	0.21
Leaf C_{mass}	0.47 (median of 79 sites)	
Root C:N ratio	94 (median of 22 sites)	
Wood C:N ratio	319 (mean of 544 individuals)	
logit NRE	$1.15 - 0.0544\,T_g + 0.282 \ln D$	0.23
Grassland		
BP	$4874 + 27.1\,T_g - 797 \ln \text{gPPFD}$	0.23
ABP/BP	0.50 (fitted by regression with zero intercept)	
Leaf C:N ratio	18 (median of 215 sites)	
Root C:N ratio	41 (median of 71 sites)	
NRE	0.69 (median of 26 sites)	

Note: Fitted models or constants are shown for biomass production (BP; $\text{g C m}^{-2}\text{year}^{-1}$); the ratio of above-ground biomass production (ABP, $\text{g C m}^{-2}\text{year}^{-1}$) to BP; the ratio of leaf biomass production (BP_{leaf}, $\text{g C m}^{-2}\text{year}^{-1}$) to ABP; leaf nitrogen per unit mass (N_{mass}, unitless); leaf carbon per unit mass (C_{mass}, unitless); root carbon-to-nitrogen ratio (C:N, g C/g N); wood carbon-to-nitrogen ratio (C:N, g C/g N) and nitrogen resorption efficiency (NRE, unitless). Site-level predictors were all mapped values (see Figure S4): soil C:N ratio (C:N, g C/g N), forest stand age (age, years), fraction of absorbed photosynthetically active radiation (fAPAR, unitless), incident photosynthetic photon flux density averaged over the growing season (gPPFD, $\mu\text{mol m}^{-2}\text{s}^{-1}$), growth temperature ($T_g$, °C), vapour pressure deficit (D, kPa), maximum rate of carboxylation at 25°C (V_{cmax25}, $\mu\text{mol m}^{-2}\text{s}^{-1}$) and leaf mass per unit area (LMA, g m^{-2}). In forests, ABP/BP, BP_{leaf}/ABP and NRE were logit-transformed and soil C:N ratio, forest stand age, gPPFD and D were log-transformed. Partial residual plots are presented in Figure 1.

light absorption. The ratio BP_{leaf}/ABP increased with fAPAR and gPPFD, but decreased with aridity. The regression models explained 44%, 17% and 8% of observed variance in forest BP, ABP/BP and BP_{leaf}/ABP, respectively (Table 1). Analyses using directly measured (instead of mapped) values of predictors showed broadly consistent patterns—with the exceptions that BP was not significantly related to measured soil C:N ratio and ABP/BP was not significantly related to gPPFD (Figure S5), probably because of the reduced sample sizes.

In grasslands, BP increased with T_g but decreased with gPPFD— qualitatively consistent with the response in forests, but explaining only 23% of observed variance. The relationship of ABP/BP to environmental variables was nonsignificant; hence, we applied a fixed ratio ABP/BP $= 0.50$ ($n = 109$).

Predictions derived from the empirical models (using site-level predictors in the data-driven model) showed general agreement with stand-scale measurements for BP ($R^2 = 0.45$: Figure 2), ABP ($R^2 = 0.44$), BBP ($R^2 = 0.16$), BP_{leaf} ($R^2 = 0.51$) and BP_{wood} ($R^2 = 0.28$) in forests; and BP ($R^2 = 0.24$), ABP ($R^2 = 0.13$) and BBP ($R^2 = 0.20$) in grasslands.

The relationship for N_{mass} as a linear function of V_{cmax25}/ LMA (Equation 2) explained 21% of the variance in observed N_{mass}. NRE was found to decrease with higher temperature and humidity; the corresponding regression model explained 23% of observed variance (Table 1).

Finally, we estimated N_{up} from the combination of BP, C allocation, tissue C:N ratios and NRE, yielding good predictions of observed N_{mass} ($R^2 = 0.39$, Figure 2i) using measured V_{cmax25} and LMA as predictors; leaf N flux ($R^2 = 0.47$, Figure 2j); NRE ($R^2 = 0.23$, Figure 2k); and N_{min} ($R^2 = 0.39$, compared with modelled N_{up} in Figure 2l) in forests.

3.2 | Global carbon and nitrogen cycling

Annual global BP was estimated as $72 \pm 14\,\text{Pg C year}^{-1}$ (Figure 3; Table S3). Modelled BP and ABP were highest in tropical and subtropical forests. This result is expected because of the year-round growing seasons in the tropics, and because both BP and ABP/BP are increased at lower soil C:N ratios and higher temperatures in these regions (Figure S4). Leaf C:N ratio was also higher in tropical forests, primarily driven by low values of V_{cmax25} at high temperatures. NRE increased towards higher latitudes, as expected because of lower temperatures.

Annual global N_{up} was estimated as $950 \pm 260\,\text{Tg N year}^{-1}$, with a global pattern similar to that of BP. Global NUE was estimated as $76 \pm 26\,\text{g C/g N}$. Global mean forest NUE was estimated as $91 \pm 37\,\text{g C/g N}$, determined by multiple climatic and soil factors. The global pattern of forest NUE differed from that of BP or N_{up}, increasing from tropical to boreal forests. Grassland NUE was assigned a constant value of $48 \pm 34\,\text{g C/g N}$, as we were unable to estimate the environmental dependencies of most components in grasslands (Table 1).
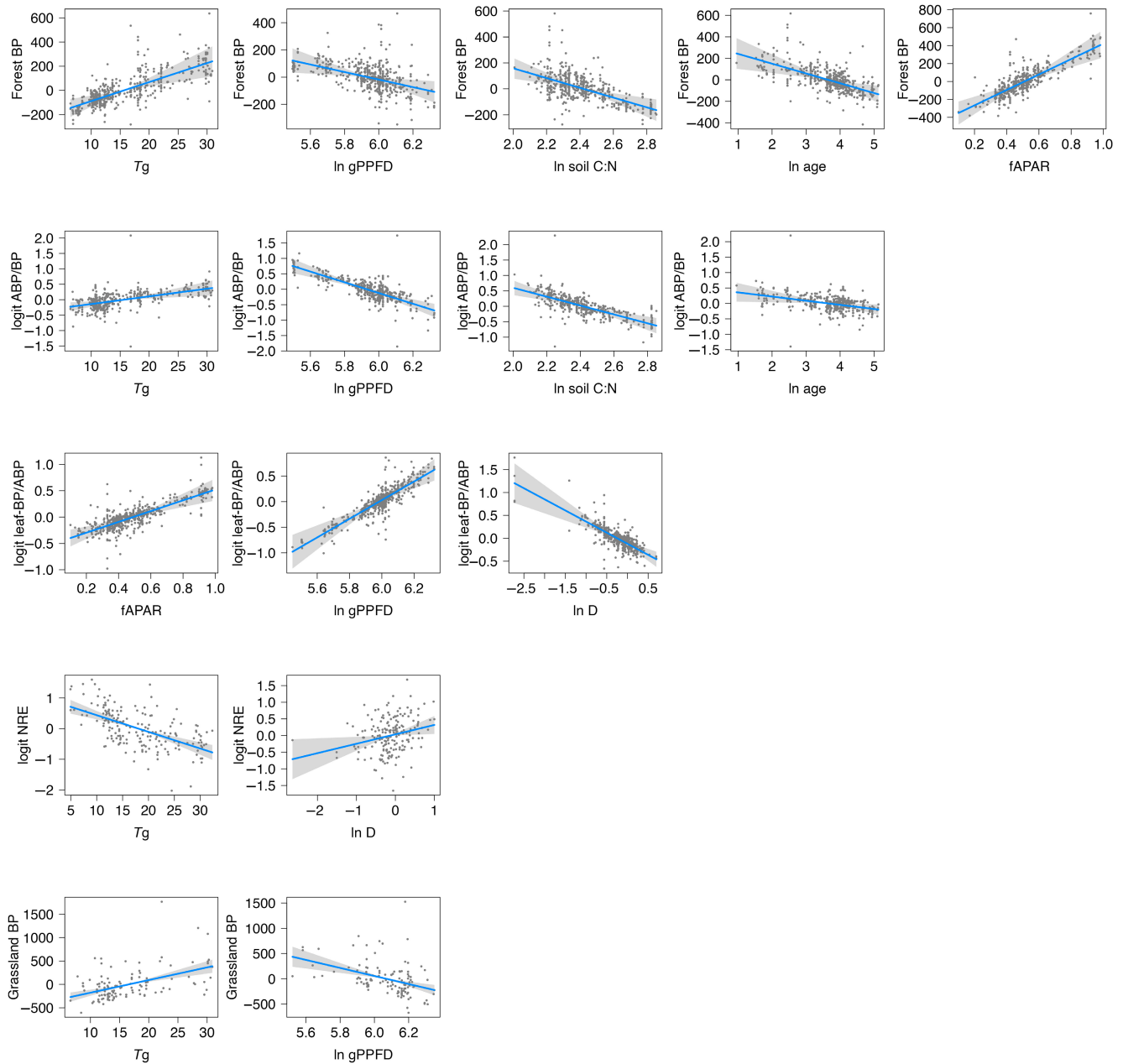
FIGURE 1 Partial residual plots for statistical models developed to predict: (1) biomass production (BP; $gCm^{-2}year^{-1}$) in forest; (2) the ratio of above-ground biomass production (ABP; $gCm^{-2}year^{-1}$) to BP; (3) the ratio of leaf biomass production (BP$_{leaf}$; $gCm^{-2}year^{-1}$) to ABP; (4) nitrogen resorption efficiency (NRE); and (5) BP in grassland. Predictors are *mapped* soil C:N, stand age, fraction of absorbed photosynthetically active radiation (fAPAR), incident photosynthetic photon flux density averaged over the growing season (gPPFD), growth temperature (T_g) and vapour pressure deficit (D). All response variables were logit-transformed, and predictors for soil C:N, age, gPPFD and D were log-transformed. Statistical models of forest BP, ABP/BP and BP$_{leaf}$/ABP used linear mixed-effects models, where site is the random intercept, and each point is represented by a measured value at ecosystem level. The statistical models for NRE and grassland BP are linear regressions, with each point representing a measured site-mean value.

3.3 | Environmental dependencies of N_{up} and NUE

The data-driven models developed here allowed us to quantify the importance of different component processes for N_{up} and NUE in forests and of variation of in modelled forest N_{up}. According to the LMG statistics, variations in BP, allocation, NRE and leaf N:C ratio and NRE, respectively, explained 45%, 22%, 22% and 11% of the variation in

modelled forest N_{up}. Climate variables (T_g, D, gPPFD) and (independently modelled, but entirely climate-driven) V_{cmax25} together explained 57% of variation in modelled forest N_{up}. fAPAR, soil C:N ratio, stand age and LMA, respectively, explained 28%, 10%, 5% and 0.6%.

Variations in allocation, leaf N:C, NRE and BP, respectively, explained 71%, 13%, 11% and 5% of the modelled variation in NUE. Climate variables and climate-derived V_{cmax25} together explained 76%
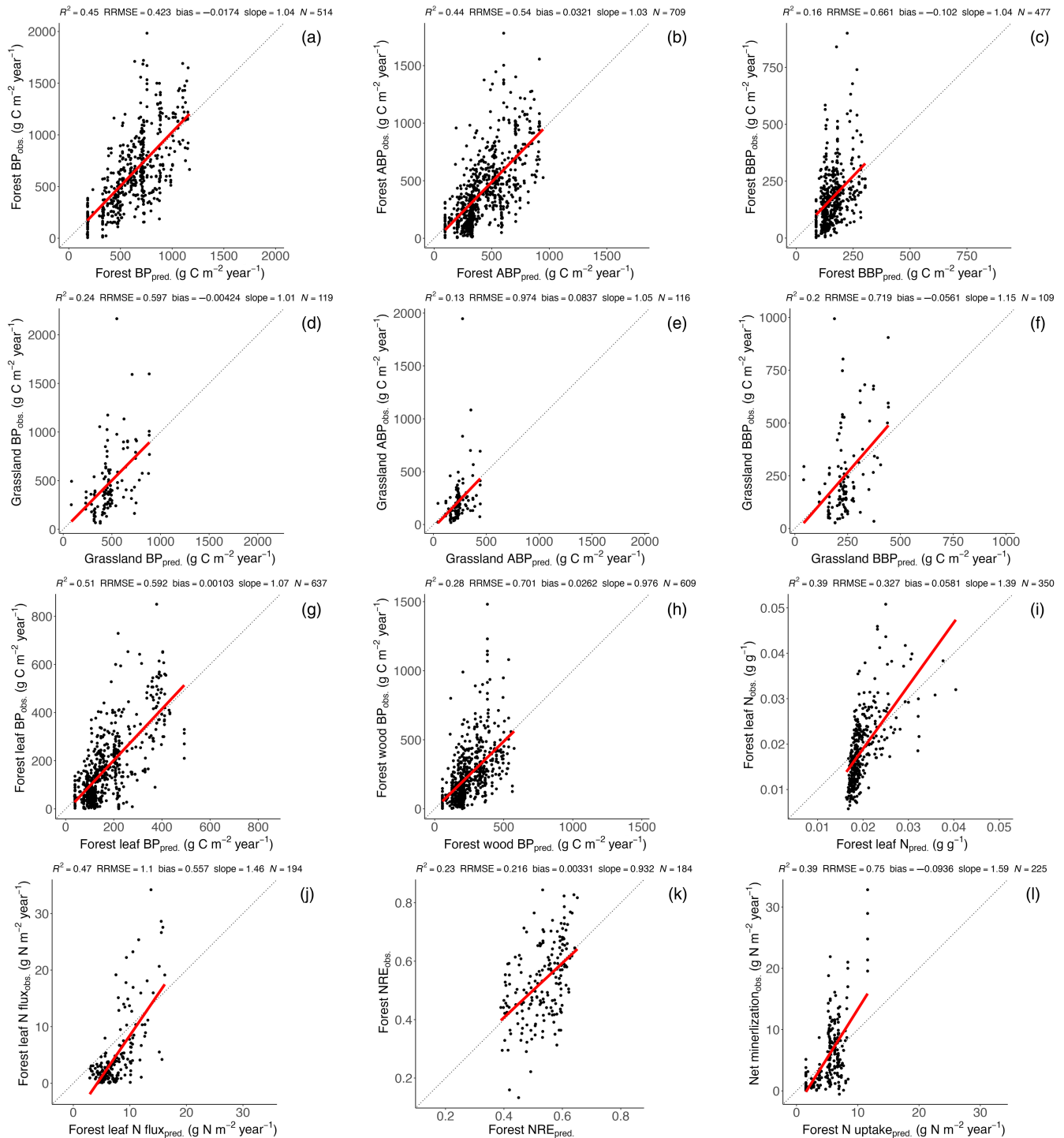
FIGURE 2 Evaluation of model predictions (see Table 1) against measurements. The dotted line is the 1:1 line. The red line represents the linear regression of modelled vs. observed values. Points in (i, k) represent site-mean values of leaf N (g g^{-1}) and nitrogen resorption efficiency (NRE, unitless). Points in (a–h, j, l) represent each individual recorded for biomass production (BP, g C m^{-2} year^{-1}), above-ground biomass production (ABP, g C m^{-2} year^{-1}), below-ground biomass production (BBP, g C m^{-2} year^{-1}), leaf biomass production (BP$_{leaf}$, g C m^{-2} year^{-1}), wood biomass production (BP$_{wood}$, g C m^{-2} year^{-1}), leaf N flux (BP$_{leaf}$ divided by leaf C:N ratio, g N m^{-2} year^{-1}) and net N mineralization (g N m^{-2} year^{-1}).

of the modelled variance in NUE. fAPAR, LMA, stand age and soil C:N, respectively, explained 16%, 5%, 2% and 1%.

Overall, we found NUE in forests to increase with LMA, age, soil C:N ratio and aridity; and to decrease with fAPAR, T_g, V_{cmax25} and

gPPFD (Table 1). The pattern of variation in NUE is dominated by climate via its effects on biomass allocation—especially allocation to leaves, which are richer in N than other tissues. Increasing leaf allocation is the primary factor leading to decreasing NUE (Figure S6).
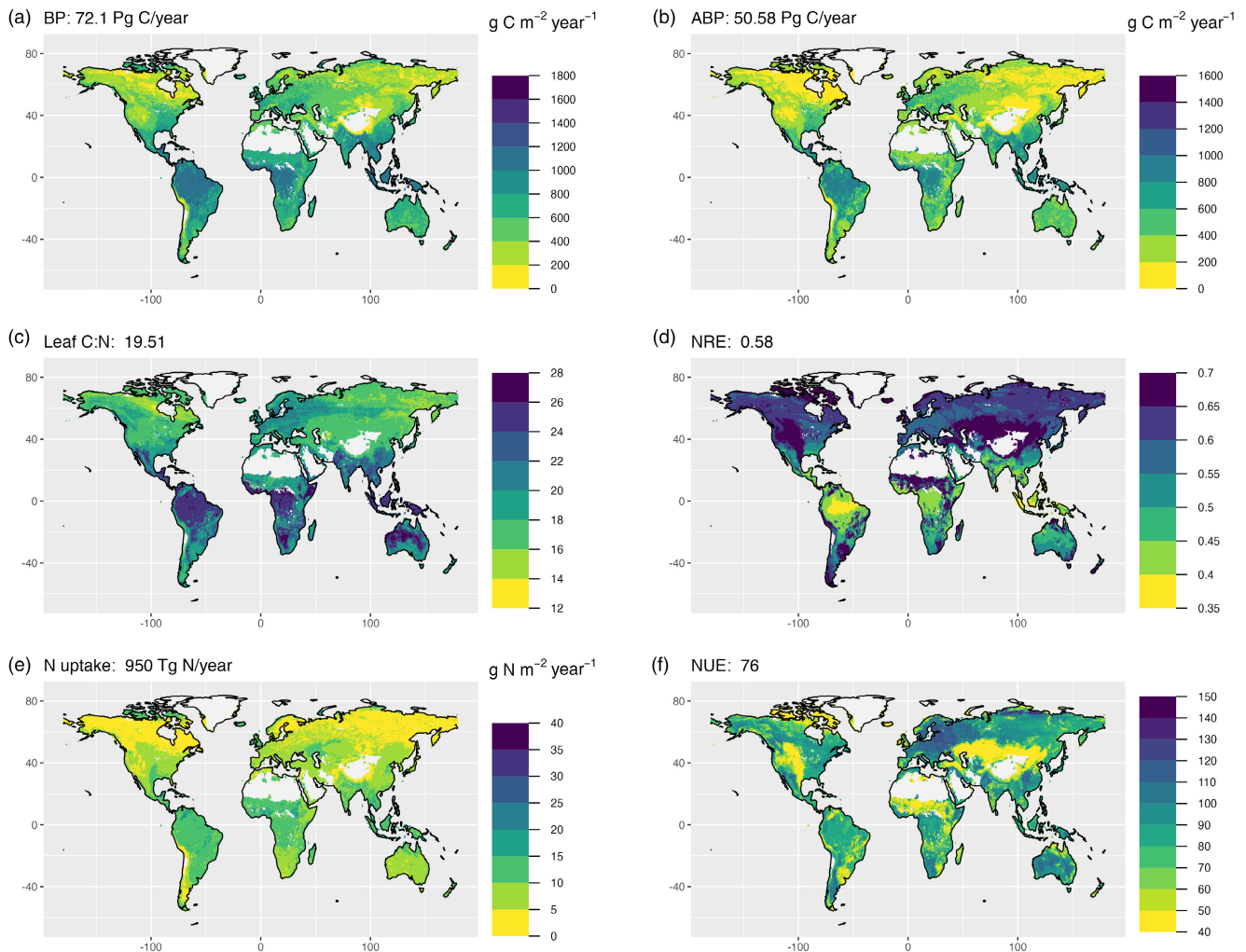
FIGURE 3 Global simulations of biomass production (BP, $g\,C\,m^{-2}\,year^{-1}$), above-ground biomass production (ABP; $g\,C\,m^{-2}\,year^{-1}$), leaf carbon-to-nitrogen ratio (leaf C:N), nitrogen resorption efficiency (NRE), N uptake ($g\,N\,m^{-2}\,year^{-1}$) and nitrogen use efficiency (NUE, the ratio of BP to N uptake). The value at the top of each panel is a global estimate. The observed sites used for fitted model and evaluation are shown in Figure S2.

Thus, NUE decreases with temperature because lower temperatures decrease above-ground allocation, including allocation to leaves; and it increases with aridity because leaf allocation is reduced in dry climates. These two patterns are compounded by the effects of NRE, which is greater in both drier and colder environments, leading to increased NUE. The decrease in NUE with gPPFD is also primarily driven by leaf allocation: increasing gPPFD decreases the ratio ABP/BP, but more importantly, increases the ratio BP_{leaf}/ABP, thereby reducing NUE.

Above-ground allocation was also reduced in soils with higher C:N ratios. However, soil C:N ratio accounted for only 1% of modelled variance in NUE, an effect much smaller than that of climate.

NUE in grassland was assigned a globally fixed value, but this value is lower than that of forests because of the high C:N ratio of wood. Low NUE in grassland explains the relatively sharp transitions (seen in Figure 3f) between low values in semiarid grasslands and much higher values in nearby dry forests.

3.4 | Comparison with global vegetation models

Comparing our global estimates with measurements for BP in forest yielded $R^2 = 0.45$ (Figure 2a). Comparison of our global estimates of N_{up} with N_{min} data yielded $R^2 = 0.39$ (Figure 2l). TRENDY models performed variably in comparison with these measurements (Table 2). Many models showed good performance, approaching that of our benchmark model, for BP. Among the four models allowing comparison with N uptake, however, none shows R^2 greater than half that of our benchmark.

We also compared the climatic dependencies of our global estimates of BP, N_{up} and NUE with TRENDY DGVMs. All the DGVMs captured the positive response of BP to temperature. Most also captured the decrease in BP with gPPFD (Figure 4). The representation of global patterns for N_{up} and NUE in relation to climate, however, showed a diversity of responses. One model showed the wrong sign for the temperature dependency of both N_{up} and NUE.

TABLE 2 Statistics for the comparison of global simulations (from our study and TRENDY output) interpolated to measurement sites. Statistics of our model were shown in bold.

	R^2	RRMSE	Rel. bias	Slope
Predicted BP vs. measured BP				
Our model	**0.45**	**0.42**	**−0.02**	**1.04**
CABLE (Haverd et al., 2018)	0.37	0.51	0.10	0.64
ISAM (Meiyappan et al., 2015)	0.36	0.52	−0.25	0.98
ISBA (Decharme et al., 2019)	0.30	0.49	−0.10	0.84
JULES (Sellar et al., 2019)	0.27	0.61	0.26	0.56
LPJ (Smith et al., 2014)	0.05	0.63	−0.23	0.45
ORCHIDEE (Goll, Vuichard, et al., 2017)	0.42	0.49	−0.21	0.92
ORCHICNP (Krinner et al., 2005)	0.12	0.57	−0.02	0.50
SDGVM (Walker et al., 2017)	0.19	0.53	−0.12	0.98
CLASS (Melton & Arora, 2016)	0.22	0.67	0.32	0.48
CLM (Lawrence et al., 2019)	0.19	0.53	−0.01	0.70
JSBACH (Mauritsen et al., 2019)	0.31	0.71	0.23	0.41
LPX (Lienert & Joos, 2018)	0.32	0.50	−0.12	0.74
Predicted N uptake vs. measured net mineralization				
Our model	**0.39**	**0.75**	**−0.09**	**1.59**
ISAM (Meiyappan et al., 2015)	0.08	0.92	−0.20	0.54
ORCHICNP (Krinner et al., 2005)	0.13	1.19	0.53	0.56
JSBACH (Mauritsen et al., 2019)	0.09	1.21	0.34	0.24
LPX (Lienert & Joos, 2018)	0.14	0.97	0.45	0.74

Note: Measured variables are biomass production (BP) and net mineralization (N_{min}). R^2 is the coefficient of determination; RRMSE is the relative root-mean-square error, as a proportion of the observed mean value; 'Rel. bias' is the difference between observed and predicted mean values, expressed as a proportion of the observed mean value; Slope is the slope of the linear regression of observed against predicted values. The site distribution is shown in Figure S2.

4 | DISCUSSION

One recent study suggested that all forest C fluxes (autotrophic respiration, NPP, above- and below-ground NPP) display similar trends with respect to latitude, temperature and growing-season length (Banbury Morgan et al., 2021), with no difference in allocation at the global scale. Many observational and experimental studies contradict this, indicating that C allocation is influenced by climate and soil factors including light (Poorter et al., 2012), water (Ma et al., 2021; Schenk & Jackson, 2002; Zhang et al., 2019), temperature (Lambers et al., 2008; Ma et al., 2021), CO_2 (Poorter et al., 2022; Terrer et al., 2018) and nutrient availability (Litton et al., 2007; Ven et al., 2019, 2020; Yan et al., 2019). Here, we focus on observed variations in BP, N_{up} and their ratio, NUE. Our analysis documents the differentiated responses of these three quantities to biotic and environmental factors, and the particular importance of variations in C allocation in determining NUE.

BP is shown to be positively related to growth temperature and light absorption, while declining with the seasonal concentration of light availability—features captured by most of the DGVMs. Additional controls on BP are soil C:N ratio (with more organic soils supporting lower BP), and forest stand age. N supply limitation on BP is well supported by observational studies (LeBauer & Treseder, 2008; Vicca et al., 2012). BP increases towards lower soil C:N ratio because higher N availability increases whole-plant photosynthesis and growth (Vicca et al., 2012). Soil C:N ratio is a relatively crude proxy for N availability (Maire et al., 2015), but it emerged here as a significant control on BP, in line with previous research (Radujković et al., 2021; Terrer et al., 2019; Van Sundert et al., 2020; Vicca et al., 2018). Regarding stand age, the longer transport pathway for water in taller trees can result in reduced stomatal conductance and photosynthesis (Drake et al., 2011) while the greater sapwood mass is required to support a given leaf area and implies increased maintenance respiration (Collalti & Prentice, 2019; Mori et al., 2010; Reich et al., 2008)—both effects potentially contributing to a decline in BP.

BP itself emerged as the most important predictor of N_{up} in our analysis—inevitably, given that N_{up} has to match the stoichiometric requirements of plant growth (Cleveland et al., 2013; Zaehle et al., 2014). This principle is therefore built into our calculation of N_{up}. Given the strong climatic controls of BP, it also follows that climate exerts a primary control on N_{up}. The involvement of soil C:N ratio as a secondary control of modelled N_{up} is consistent with soil N limitations on whole-plant C and N uptake (Lawrence et al., 2019; Mauritsen et al., 2019).

The ratio of ABP to BP showed responses to the environment that are qualitatively similar to those of BP, including similar responses to soil C:N ratio—indicating that less fertile soil conditions tend to increase BBP relative to ABP. From high to low soil N availability, as indicated here by increasing soil C:N ratio, increasing allocation of C to roots is commonly observed along with decreasing allocation to above-ground production (Franklin et al., 2012; Peng et al., 2017). The large below-ground C allocation in soils with low N availability reflects greater investments into N_{up} through enhanced fine root production. This might also be accompanied by greater investments into ectomycorrhizal (ECM) fungi to acquire N from soil organic matter (Phillips et al., 2013), causing accelerated soil C turnover (Pregitzer et al., 2008) and N cycling (Zak et al., 2011). The component of C exported to mycorrhizae and exuded into the soil is not contained in BP_{root}, BBP and BP and is rarely measured, but a potentially substantial component of NPP (Vicca et al., 2012).

The ratio of BP_{leaf} to ABP in forests increases with moisture, here measured by the growing-season mean vapour pressure deficit, probably because sapwood area per unit leaf area increases with aridity because of the additional water requirement of a given rate of photosynthesis under dry conditions (Mencuccini & Grace, 1995). The positive effect of fAPAR on this ratio is expected, because of the direct link between leaf light absorption and photosynthesis. The positive effect of gPPFD might reflect the fact that the annual C allocation to leaves is determined by the annual maximum foliage: A shorter growing season allows each unit of leaf carbon to produce less photosynthate and therefore likely less BP.
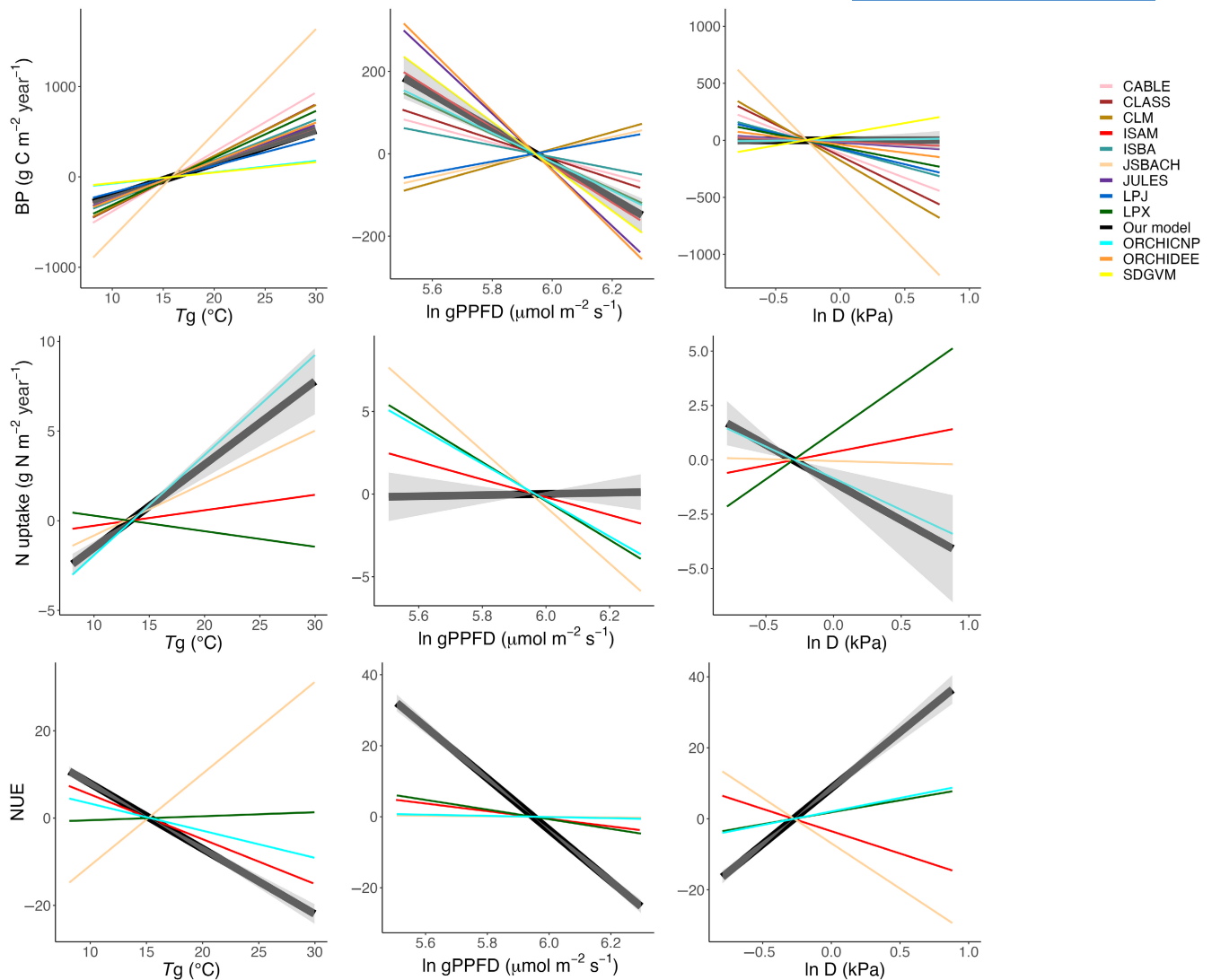
FIGURE 4 Partial residual relationships for modelled biomass production (BP, $g\,C\,m^{-2}\,year^{-1}$), N uptake (N_{up}, $g\,N\,m^{-2}\,year^{-1}$) and nitrogen use efficiency (NUE, $g\,C/g\,N$) as functions of incident photosynthetic photon flux density averaged over the growing season (gPPFD, $\mu mol\,m^{-2}\,s^{-1}$), growth temperature (T_g, °C) and vapour pressure deficit (D, kPa) during the thermal growing season. Predicted site-level BP was based on all measured BP plots in forests; predicted site-level N_{up} was based on all measured N mineralization plots in forests; predicted site-level NUE was based on all measured BP and N mineralization plots in forest (Figure S2a, e).

Tissue stoichiometry and NRE explained less variance in N_{up} than BP and biomass allocation (Wang, Ciais, et al., 2018). Modelled leaf C:N ratios decreased towards high latitudes, driven by V_{cmax25} increasing towards cold climates (Peng et al., 2021). This pattern is consistent with the principle of the LPJ-GUESS model (Smith et al., 2014), which assumes that leaf N is driven by its climate-driven demand rather than soil N supply. It is not captured by models wherein leaf C:N ratio is assigned PFT-specific (Lawrence et al., 2019; Oleson et al., 2010) or globally fixed (Wiltshire et al., 2021) values.

Global mean NRE was shown to increase from low to high latitudes, driven by negative effects of temperature and humidity on NRE. Because rates of N cycling are enhanced in warmer and wetter environments, N supply from resorption is relatively less important in tropical regions relative to higher latitudes (Deng et al., 2018; Du et al., 2020).

Our analysis casts some light on the opposition between 'biogeochemical niche differentiation' (Peñuelas et al., 2019; Sardans et al., 2021) and 'climate-driven demand' (Wang, Ciais, et al., 2018) as the primary controls of ecosystem stoichiometry. Globally, soil C:N ratio accounted for just 10% of the modelled variation in N_{up} and 1% of the modelled variation in NUE. N deposition was initially considered as an additional predictor for BP and allocation, but produced no improvement in the fitted model performance for N_{up} and was therefore discarded for the further analysis and modelling. By contrast, climate accounted for 57% of modelled variation in N_{up} and 76% of modelled variation in NUE. These results point to a dominant control of N_{up} and NUE by climate, with a secondary influence by soils. However, soils are linked to climate through their development (Jenny, 1994); soil and climate variables are thus not statistically independent. In combination with the small-scale heterogeneity

of soils and shortcomings of global soil data in capturing this, the emergence of climate-related variables as dominant over soil factors in global statistical analyses like ours should be interpreted with caution.

Overall, biomass allocation emerged as the dominant process controlling of forest NUE (driving 71% of modelled variance). This finding is consistent with GOLUM-CNP (Wang, Ciais, et al., 2018), where biomass allocation explained >80% of modelled variation in NUE (defined as the ratio of gross primary production to N_{up} in their study). According to our models, forest NUE is primarily driven by climate, increasing towards colder and drier climates. A possible interpretation of this pattern invokes the concept that high efficiency of resource use is favoured when resource supplies are more limiting to production (Harrington et al., 2001). This interpretation is supported by observations (Gill & Finzi, 2016) and simulations (Wang, Ciais, et al., 2018), indicating that NUE increases from tropical to boreal forest. In boreal forests, much of the N pool is bound to organic material and is depolymerized by microbially produced hydrolytic and oxidative enzymes whose activity is limited by low temperatures (Gill & Finzi, 2016). To overcome this limitation, boreal plants are dependent on ECM or ericoid microbial symbioses for efficient N acquisition (Högberg et al., 2010; Näsholm, 1998; Terrer et al., 2019), requiring greater C allocation below ground (Gill & Finzi, 2016). The increase in NUE with aridity can be explained by reduced allocation to (N-rich) leaves. NRE also plays a role, as N conservation (by resorption) is a favoured strategy in colder and drier environments.

Globally, however, the lowest NUE according to our mapping is encountered in arid regions (including Central Asia, the interior West of North America and the Sahel) where grasslands dominate. The highest NUE is shown primarily in temperate forests, especially in northern Europe and China, where relatively low temperatures increase below-ground allocation and decrease NRE. N deposition in these regions is among the highest globally (Reay et al., 2008), suggesting that N deposition is not a primary control on NUE. Much of Australia is also shown as a region of high NUE because of the occurrence of forests in dry climates that favour reduced leaf allocation and high NRE.

The increase in NUE from tropical to boreal forest has also been linked to decreasing soil N supply or soil N:P ratio (Gill & Finzi, 2016). In our analysis, soil C:N ratio accounted for 10% of overall variance for N_{up} but only 1% for NUE, suggesting that soil N supply is a minor factor determining NUE and implying that effects of climate—which include indirect effects, such as the increased C cost of N acquisition at low temperatures—are dominant.

Existing coupled C–N cycle models predict plant C allocation by a variety of methods. Some assume fixed (PFT-specific) allocation fractions; others embed functional relationships between different dimensions, such as leaf and sapwood area (Zaehle et al., 2014), in more process-based formulations. Some analyses have used satellite observations of LAI and above-ground biomass (CARDAMOM; Bloom et al., 2016) directly as inputs. Given the importance of C allocation for the N cycle, it is important to check that assumptions made about C allocation are realistic. This is not always the case. For example, Wang, Ciais, et al. (2018) noted that in CARDAMOM, allocation to wood production was commonly >60% (this is rare in measurements) and that the turnover time of leaves in temperate and boreal biomes was <1 year (but for evergreen leaves it is commonly 2.5–10 years). Different assumptions about C allocation will necessarily lead to divergent estimations of NUE, so the present situation implies huge uncertainty about the patterns and controls of NUE that could be reduced by systematic comparison against observationally based benchmarks.

We have noted that the distinction between forest and grassland distributions is an important factor determining NUE in our global maps. Our approach is consistent with TRENDY models that assign PFT-specific leaf C:N ratios, C allocation fractions and NRE (Smith et al., 2014; Wiltshire et al., 2021). Nonetheless, it is simplistic in (a) assuming sharp boundaries and (b) assigning fixed values to several parameters for grasslands. More work is required to improve the estimation of plant properties related to N cycling in nonforest biomes.

Global BP was estimated as $72 \pm 14 \, \text{Pg C year}^{-1}$, larger than in earlier studies by Cleveland et al. (2013; $44.35 \, \text{Pg C year}^{-1}$) and Wang, Ciais, et al. (2018; $52.50 \, \text{Pg C year}^{-1}$). Global total N_{up} was estimated as $950 \pm 260 \, \text{Tg N year}^{-1}$. This falls towards the upper end of the range of estimates by six models of global C and N cycling: 465 (Wiltshire et al., 2021), 728 (Smith et al., 2014), 831 (Goll, Winkler, et al., 2017), 968 (Oleson et al., 2010), 1172 (Lawrence et al., 2019) and $1197 \, \text{Tg N year}^{-1}$ (Cleveland et al., 2013). Global NUE was estimated as $76 \pm 26 \, \text{g C/g N}$. This falls within the range estimated by other models: $50 \, \text{g C/g N}$ by the TEM model (Melillo et al., 1993), $52 \, \text{g C/g N}$ by the O-CN model (Zaehle et al., 2010), $56 \, \text{g C/g N}$ by the ORCHIDEE model (Goll, Vuichard, et al., 2017) and $80 \, \text{g C/g N}$ by the ISAM model (Meiyappan et al., 2015). Thus, our central estimates of global N_{up} and NUE are within the broad ranges simulated by current models. To further improve the reliability of the global N uptake flux, data limitations will have to be resolved, in particular for root N concentrations and the distinction between below-ground biomass production of fine and coarse roots. The latter posed a limitation to considering their distinct C:N ratios in the analysis here—with unclear implications for a potential bias in our estimates of the N requirement for BP_{root}.

In conclusion, our data-driven modelling approach has generated quantitative relationships that are broadly consistent with experimental and observational evidence for the controls of different processes contributing to the coupling of the terrestrial C and N cycles. Data on nonforest ecosystems are, however sparse, limiting the information that can be derived from them. Further limitations of this study include relatively low R^2 values for some comparisons (especially those related to C allocation to different tissues), and the lack of available measurements of soil factors more directly related to plant function than soil C:N ratio, a relatively crude metric of N availability. Despite these limitations, our analysis provides new benchmarks for coupled C–N cycle modelling. We have presented initial comparisons with TRENDY model simulations, based on their

publicly available outputs. Simplified representations of allocation and tissue C:N ratios in TRENDY models might be responsible for divergence of the modelled N_{up} and NUE responses to climate from one another, and from the benchmarks provided here. A more in-depth examination of model behaviour would be worthwhile in the light of our findings, potentially contributing to a reduction in the uncertainties associated with N cycle constraints on ecosystem C uptake in a changing environment.

AUTHOR CONTRIBUTIONS

ACKNOWLEDGEMENTS

CONFLICT OF INTEREST STATEMENT

The authors declare no competing interests.

PEER REVIEW

The peer review history for this article is available at https://www.webofscience.com/api/gateway/wos/peer-review/10.1111/1365-2745.14208.

DATA AVAILABILITY STATEMENT

No new data were used in the analysis and models presented here. The observed data for biomass production, C and N allocation, tissue C:N ratios and N resorption efficiency were collected from the cited publications. Data and code used for analyses are available via Zenodo https://doi.org/10.5281/zenodo.8182205 (Peng, 2023).

ORCID

Yunke Peng https://orcid.org/0000-0001-5240-0725

REFERENCES

Anderson-Teixeira, K. J., Wang, M. M. H., McGarvey, J. C., Herrmann, V., Tepley, A. J., Bond-Lamberty, B., & LeBauer, D. S. (2018). ForC: A global database of forest carbon stocks and fluxes. *Ecology*, *99*(6), 1507. https://doi.org/10.1002/ecy.2229

Anderson-Teixeira, K. J., Wang, M. M. H., McGarvey, J. C., & LeBauer, D. S. (2016). Carbon dynamics of mature and regrowth tropical forests derived from a pantropical database (TropForC-db). *Global Change Biology*, *22*(5), 1690–1709. https://doi.org/10.1111/gcb.13226

Arora, V. K., Katavouta, A., Williams, R. G., Jones, C. D., Brovkin, V., Friedlingstein, P., Schwinger, J., Bopp, L., Boucher, O., Cadule, P., Chamberlain, M. A., Christian, J. R., Delire, C., Fisher, A. R. A., Hajima, T., Ilyina, T., Joetzjer, E., Kawamiya, M., Koven, C. D., … Ziehn, T. (2020). Carbon-concentration and carbon-climate feedbacks in CMIP6 models and their comparison to CMIP5 models. *Biogeosciences*, *17*(16), 4173–4222. https://doi.org/10.5194/bg-17-4173-2020

Atkin, O. K., Bloomfield, K. J., Reich, P. B., Tjoelker, M. G., Asner, G. P., Bonal, D., Bönisch, G., Bradford, M. G., Cernusak, L. A., Cosio, E. G., Creek, D., Crous, K. Y., Domingues, T. F., Dukes, J. S., Egerton, J. J. G., Evans, J. R., Farquhar, G. D., Fyllas, N. M., Gauthier, P. P. G., … Zaragoza-Castells, J. (2015). Global variability in leaf respiration in relation to climate, plant functional types and leaf traits. *New Phytologist*, *206*(2), 614–636. https://doi.org/10.1111/nph.13253

Bahar, N. H. A., Ishida, F. Y., Weerasinghe, L. K., Guerrieri, R., O'Sullivan, O. S., Bloomfield, K. J., Asner, G. P., Martin, R. E., Lloyd, J., Malhi, Y., Phillips, O. L., Meir, P., Salinas, N., Cosio, E. G., Domingues, T. F., Quesada, C. A., Sinca, F., Escudero Vega, A., Zuloaga Ccorimanya, P. P., … Atkin, O. K. (2017). Leaf-level photosynthetic capacity in low-land Amazonian and high-elevation Andean tropical moist forests of Peru. *New Phytologist*, *214*(3), 1002–1018. https://doi.org/10.1111/nph.14079

Baig, S., Medlyn, B. E., Mercado, L. M., & Zaehle, S. (2015). Does the growth response of woody plants to elevated CO_2 increase with temperature? A model-oriented meta-analysis. *Global Change Biology*, *21*(12), 4303–4319. https://doi.org/10.1111/gcb.12962

Banbury Morgan, R., Herrmann, V., Kunert, N., Bond-Lamberty, B., Muller-Landau, H. C., & Anderson-Teixeira, K. J. (2021). Global patterns of forest autotrophic carbon fluxes. *Global Change Biology*, *27*(12), 2840–2855. https://doi.org/10.1111/gcb.15574

Batjes, N. H. (2015). *World soil property estimates for broad-scale modelling (WISE30sec)* (No. 2015/01). ISRIC-World Soil Information.

Bernacchi, C. J., Singsaas, E. L., Pimentel, C., Portis, A. R., & Long, S. P. (2001). Improved temperature response functions for models of Rubisco-limited photosynthesis. *Plant, Cell and Environment*, *24*(2), 253–259. https://doi.org/10.1046/j.1365-3040.2001.00668.x

Bloom, A. A., Exbrayat, J. F., Van Der Velde, I. R., Feng, L., & Williams, M. (2016). The decadal state of the terrestrial carbon cycle: Global retrievals of terrestrial carbon allocation, pools, and residence times. *Proceedings of the National Academy of Sciences of the United States of America*, *113*(5), 1285–1290. https://doi.org/10.1073/pnas.1515160113

Bloomfield, K. J., Prentice, I. C., Cernusak, L. A., Eamus, D., Medlyn, B. E., Rumman, R., Wright, I. J., Boer, M. M., Cale, P., Cleverly, J., Egerton, J. J. G., Ellsworth, D. S., Evans, B. J., Hayes, L. S., Hutchinson, M. F., Liddell, M. J., Macfarlane, C., Meyer, W. S., Togashi, H. F., … Atkin, O. K. (2019). The validity of optimal leaf traits modelled on environmental conditions. *New Phytologist*, *221*(3), 1409–1423. https://doi.org/10.1111/nph.15495

Campioli, M., Vicca, S., Luyssaert, S., Bilcke, J., Ceschia, E., Chapin, F. S., Ciais, P., Fernández-Martínez, M., Malhi, Y., Obersteiner, M., Olefeldt, D., Papale, D., Piao, S. L., Peñuelas, J., Sullivan, P. F., Wang, X., Zenone, T.,

& Janssens, I. A. (2015). Biomass production efficiency controlled by management in temperate and boreal ecosystems. *Nature Geoscience*, *8*(11), 843–846. https://doi.org/10.1038/ngeo2553

Cernusak, L. A., Hutley, L. B., Beringer, J., Holtum, J. A. M., & Turner, B. L. (2011). Photosynthetic physiology of eucalypts along a sub-continental rainfall gradient in northern Australia. *Agricultural and Forest Meteorology*, *151*(11), 1462–1470. https://doi.org/10.1016/j.agrformet.2011.01.006

Cleveland, C. C., Houlton, B. Z., Smith, W. K., Marklein, A. R., Reed, S. C., Parton, W., Del Grosso, S. J., & Running, S. W. (2013). Patterns of new versus recycled primary production in the terrestrial biosphere. *Proceedings of the National Academy of Sciences of the United States of America*, *110*(31), 12733–12737. https://doi.org/10.1073/pnas.1302768110

Collalti, A., Ibrom, A., Stockmarr, A., Cescatti, A., Alkama, R., Fernández-Martínez, M., Matteucci, G., Sitch, S., Friedlingstein, P., Ciais, P., Goll, D. S., Nabel, J. E. M. S., Pongratz, J., Arneth, A., Haverd, V., & Prentice, I. C. (2020). Forest production efficiency increases with growth temperature. *Nature Communications*, *11*(1), 1–9. https://doi.org/10.1038/s41467-020-19187-w

Collalti, A., & Prentice, I. C. (2019). Is NPP proportional to GPP? Waring's hypothesis 20 years on. *Tree Physiology*, *39*(8), 1473–1483. https://doi.org/10.1093/treephys/tpz034

Davies-Barnard, T., Meyerholt, J., Zaehle, S., Friedlingstein, P., Brovkin, V., Fan, Y., Fisher, R. A., Jones, C. D., Lee, H., Peano, D., Smith, B., Wärlind, D., & Wiltshire, A. J. (2020). Nitrogen cycling in CMIP6 land surface models: Progress and limitations. *Biogeosciences*, *17*(20), 5129–5148. https://doi.org/10.5194/bg-17-5129-2020

Decharme, B., Delire, C., Minvielle, M., Colin, J., Vergnes, J. P., Alias, A., Saint-Martin, D., Séférian, R., Sénési, S., & Voldoire, A. (2019). Recent changes in the ISBA-CTRIP land surface system for use in the CNRM-CM6 climate model and in global off-line hydrological applications. *Journal of Advances in Modeling Earth Systems*, *11*(5), 1207–1252. https://doi.org/10.1029/2018MS001545

Deng, M., Liu, L., Jiang, L., Liu, W., Wang, X., Li, S., Yang, S., & Wang, B. (2018). Ecosystem scale trade-off in nitrogen acquisition pathways. *Nature Ecology & Evolution*, *2*(11), 1724–1734. https://doi.org/10.1038/s41559-018-0677-1

Domingues, T. F., Ishida, F. Y., Feldpausch, T. R., Grace, J., Meir, P., Saiz, G., Sene, O., Schrodt, F., Sonké, B., Taedoumg, H., Veenendaal, E. M., Lewis, S., & Lloyd, J. (2015). Biome-specific effects of nitrogen and phosphorus on the photosynthetic characteristics of trees at a forest-savanna boundary in Cameroon. *Oecologia*, *178*(3), 659–672. https://doi.org/10.1007/s00442-015-3250-5

Domingues, T. F., Meir, P., Feldpausch, T. R., Saiz, G., Veenendaal, E. M., Schrodt, F., Bird, M., Djagbletey, G., Hien, F., Compaore, H., Diallo, A., Grace, J., & Lloyd, J. (2010). Co-limitation of photosynthetic capacity by nitrogen and phosphorus in West Africa woodlands. *Plant, Cell and Environment*, *33*(6), 959–980. https://doi.org/10.1111/j.1365-3040.2010.02119.x

Dong, N., Prentice, I. C., Evans, B. J., Caddy-Retalic, S., Lowe, A. J., & Wright, I. J. (2017). Leaf nitrogen from first principles: Field evidence for adaptive variation with climate. *Biogeosciences*, *14*(2), 481–495. https://doi.org/10.5194/bg-14-481-2017

Dong, N., Prentice, I. C., Wright, I. J., Wang, H., Atkin, O. K., Bloomfield, K. J., Domingues, T. F., Gleason, S. M., Maire, V., Onoda, Y., Poorter, H., & Smith, N. G. (2022). Leaf nitrogen from the perspective of optimal plant function. *Journal of Ecology*, *110*(11), 2585–2602. https://doi.org/10.1111/1365-2745.13967

Dong, N., Wright, I. J., Chen, J. M., Luo, X., Wang, H., Keenan, T. F., Smith, N. G., & Prentice, I. C. (2022). Rising CO_2 and warming reduce global canopy demand for nitrogen. *New Phytologist*, *235*(5), 1692–1700. https://doi.org/10.1111/nph.18076

Drake, J. E., Davis, S. C., Raetz, L. M., & Delucia, E. H. (2011). Mechanisms of age-related changes in forest production: The influence of

physiological and successional changes. *Global Change Biology*, *17*(4), 1522–1535. https://doi.org/10.1111/j.1365-2486.2010.02342.x

Du, E., Terrer, C., Pellegrini, A. F. A., Ahlström, A., van Lissa, C. J., Zhao, X., Xia, N., Wu, X., & Jackson, R. B. (2020). Global patterns of terrestrial nitrogen and phosphorus limitation. *Nature Geoscience*, *13*(3), 221–226. https://doi.org/10.1038/s41561-019-0530-4

Fay, P. A., Prober, S. M., Harpole, W. S., Knops, J. M. H., Bakker, J. D., Borer, E. T., Lind, E. M., MacDougall, A. S., Seabloom, E. W., Wragg, P. D., Adler, P. B., Blumenthal, D. M., Buckley, Y. M., Chu, C., Cleland, E. E., Collins, S. L., Davies, K. F., Du, G., Feng, X., … Yang, L. H. (2015). Grassland productivity limited by multiple nutrients. *Nature Plants*, *1*(7), 1–5. https://doi.org/10.1038/nplants.2015.80

Finzi, A. C., Norby, R. J., Calfapietra, C., Gallet-Budynek, A., Gielen, B., Holmes, W. E., Hoosbeek, M. R., Iversen, C. M., Jackson, R. B., Kubiske, M. E., Ledford, J., Liberloo, M., Oren, R., Polle, A., Pritchard, S., Zak, D. R., Schlesinger, W. H., & Ceulemans, R. (2007). Increases in nitrogen uptake rather than nitrogen-use efficiency support higher rates of temperate forest productivity under elevated CO_2. *Proceedings of the National Academy of Sciences of the United States of America*, *104*(35), 14014–14019. https://doi.org/10.1073/pnas.0706518104

Fowler, D., Steadman, C. E., Stevenson, D., Coyle, M., Rees, R. M., Skiba, U. M., Sutton, M. A., Cape, J. N., Dore, A. J., Vieno, M., Simpson, D., Zaehle, S., Stocker, B. D., Rinaldi, M., Facchini, M. C., Flechard, C. R., Nemitz, E., Twigg, M., Erisman, J. W., … Galloway, J. N. (2015). Effects of global change during the 21st century on the nitrogen cycle. *Atmospheric Chemistry and Physics*, *15*(24), 13849–13893. https://doi.org/10.5194/acp-15-13849-2015

Franklin, O., Johansson, J., Dewar, R. C., Dieckmann, U., McMurtrie, R. E., Brännström, A. K., & Dybzinski, R. (2012). Modeling carbon allocation in trees: A search for principles. *Tree Physiology*, *32*(6), 648–666. https://doi.org/10.1093/treephys/tpr138

Friedlingstein, P., Jones, M. W., O'sullivan, M., Andrew, R. M., Hauck, J., Peters, G. P., Peters, W., Pongratz, J., Sitch, S., Le Quéré, C., Bakker, D. C. E., Canadell, J. G., Ciais, P., Jackson, R. B., Anthoni, P., Barbero, L., Bastos, A., Bastrikov, V., Becker, M., … Zaehle, S. (2019). Global carbon budget 2019. *Earth System Science Data*, *11*(4), 1783–1838. https://doi.org/10.5194/essd-11-1783-2019

Gill, A. L., & Finzi, A. C. (2016). Belowground carbon flux links biogeochemical cycles and resource-use efficiency at the global scale. *Ecology Letters*, *19*(12), 1419–1428. https://doi.org/10.1111/ele.12690

Goll, D. S., Vuichard, N., Maignan, F., Jornet-Puig, A., Sardans, J., Violette, A., Peng, S., Sun, Y., Kvakic, M., Guimberteau, M., Guenet, B., Zaehle, S., Penuelas, J., Janssens, I., & Ciais, P. (2017). A representation of the phosphorus cycle for ORCHIDEE (revision 4520). *Geoscientific Model Development*, *10*(10), 3745–3770. https://doi.org/10.5194/gmd-10-3745-2017

Goll, D. S., Winkler, A. J., Raddatz, T., Dong, N., Colin Prentice, I., Ciais, P., & Brovkin, V. (2017). Carbon-nitrogen interactions in idealized simulations with JSBACH (version 3.10). *Geoscientific Model Development*, *10*(5), 2009–2030. https://doi.org/10.5194/gmd-10-2009-2017

Grömping, U. (2006). Relative importance for linear regression in R: The package relaimpo. *Journal of Statistical Software*, *17*(1), 1–27. https://doi.org/10.18637/jss.v017.i01

Harrington, R. A., Fownes, J. H., & Vitousek, P. M. (2001). Production and resource use efficiencies in N- and P-limited tropical forests: A comparison of responses to long-term fertilization. *Ecosystems*, *4*(7), 646–657. https://doi.org/10.1007/s10021-001-0034-z

Harris, I., Jones, P. D., Osborn, T. J., & Lister, D. H. (2014). Updated high-resolution grids of monthly climatic observations—The CRU TS3.10 dataset. *International Journal of Climatology*, *34*(3), 623–642. https://doi.org/10.1002/joc.3711

Harrison, M. T., Edwards, E. J., Farquhar, G. D., Nicotra, A. B., & Evans, J. R. (2009). Nitrogen in cell walls of sclerophyllous leaves accounts for little of the variation in photosynthetic nitrogen-use

efficiency. *Plant, Cell and Environment*, 32(3), 259–270. https://doi.org/10.1111/j.1365-3040.2008.01918.x

Haverd, V., Smith, B., Nieradzik, L., Briggs, P. R., Woodgate, W., Trudinger, C. M., Canadell, J. G., & Cuntz, M. (2018). A new version of the CABLE land surface model (subversion revision r4601) incorporating land use and land cover change, woody vegetation demography, and a novel optimisation-based approach to plant coordination of photosynthesis. *Geoscientific Model Development*, 11(7), 2995–3026. https://doi.org/10.5194/gmd-11-2995-2018

Henneron, L., Kardol, P., Wardle, D. A., Cros, C., & Fontaine, S. (2020). Rhizosphere control of soil nitrogen cycling: A key component of plant economic strategies. *New Phytologist*, 228(4), 1269–1282. https://doi.org/10.1111/nph.16760

Högberg, M. N., Briones, M. J. I., Keel, S. G., Metcalfe, D. B., Campbell, C., Midwood, A. J., Thornton, B., Hurry, V., Linder, S., Näsholm, T., & Högberg, P. (2010). Quantification of effects of season and nitrogen supply on tree below-ground carbon transfer to ectomycorrhizal fungi and other soil organisms in a boreal pine forest. *New Phytologist*, 187(2), 485–493. https://doi.org/10.1111/j.1469-8137.2010.03274.x

Hungate, B. A., Dukes, J. S., Shaw, M. R., Luo, Y., & Field, C. B. (2003). Nitrogen and climate change. *Science*, 302(5650), 1512–1513. https://doi.org/10.1126/science.1091390

Jenny, H. (1994). *Factors of soil formation: A system of quantitative pedology*. Courier Corporation.

Jones, H. G. (2013). *Plants and microclimate: A quantitative approach to environmental plant physiology*. Cambridge University Press.

Krinner, G., Viovy, N., de Noblet-Ducoudré, N., Ogée, J., Polcher, J., Friedlingstein, P., Ciais, P., Sitch, S., & Prentice, I. C. (2005). A dynamic global vegetation model for studies of the coupled atmosphere-biosphere system. *Global Biogeochemical Cycles*, 19(1), 1–33. https://doi.org/10.1029/2003GB002199

Lambers, H., Chapin, F. S., III, & Pons, T. L. (2008). *Plant physiological ecology*. Springer.

Lawrence, D. M., Fisher, R. A., Koven, C. D., Oleson, K. W., Swenson, S. C., Bonan, G., Collier, N., Ghimire, B., van Kampenhout, L., Kennedy, D., Kluzek, E., Lawrence, P. J., Li, F., Li, H., Lombardozzi, D., Riley, W. J., Sacks, W. J., Shi, M., Vertenstein, M., … Zeng, X. (2019). The community land model version 5: Description of new features, benchmarking, and impact of forcing uncertainty. *Journal of Advances in Modeling Earth Systems*, 11(12), 4245–4287. https://doi.org/10.1029/2018MS001583

Le Quéré, C., Andrew, R. M., Friedlingstein, P., Sitch, S., Pongratz, J., Manning, A. C., Korsbakken, J. I., Peters, G. P., Canadell, J. G., Jackson, R. B., Boden, T. A., Tans, P. P., Andrews, O. D., Arora, V. K., Bakker, D. C. E., Barbero, L., Becker, M., Betts, R. A., Bopp, L., … Zhu, D. (2018). Global carbon budget 2018. *Earth System Science Data*, 10(4), 2141–2194. https://doi.org/10.5194/essd-10-2141-2018

LeBauer, D. S., & Treseder, K. K. (2008). Nitrogen limitation of net primary productivity in terrestrial ecosystems is globally distributed. *Ecology*, 89(2), 371–379. https://doi.org/10.1890/06-2057.1

Liang, X., Zhang, T., Lu, X., Ellsworth, D. S., BassiriRad, H., You, C., Wang, D., He, P., Deng, Q., Liu, H., Mo, J., & Ye, Q. (2020). Global response patterns of plant photosynthesis to nitrogen addition: A meta-analysis. *Global Change Biology*, 26(6), 3585–3600. https://doi.org/10.1111/gcb.15071

Lienert, S., & Joos, F. (2018). A Bayesian ensemble data assimilation to constrain model parameters and land-use carbon emissions. *Biogeosciences*, 15(9), 2909–2930. https://doi.org/10.5194/bg-15-2909-2018

Litton, C. M., Raich, J. W., & Ryan, M. G. (2007). Carbon allocation in forest ecosystems. *Global Change Biology*, 13(10), 2089–2109. https://doi.org/10.1111/j.1365-2486.2007.01420.x

Liu, M., Li, C., Xu, X., Wanek, W., Jiang, N., Wang, H., & Yang, X. (2017). Organic and inorganic nitrogen uptake by 21 dominant tree species in temperate and tropical forests. *Tree Physiology*, 37(11), 1515–1526. https://doi.org/10.1093/treephys/tpx046

Luo, X., Keenan, T. F., Chen, J. M., Croft, H., Colin Prentice, I., Smith, N. G., Walker, A. P., Wang, H., Wang, R., Xu, C., & Zhang, Y. (2021). Global variation in the fraction of leaf nitrogen allocated to photosynthesis. *Nature Communications*, 12(1), 1–10. https://doi.org/10.1038/s41467-021-25163-9

Luyssaert, S., Inglima, I., Jung, M., Richardson, A. D., Reichstein, M., Papale, D., Piao, S. L., Schulze, E. D., Wingate, L., Matteucci, G., Aragao, L., Aubinet, M., Beer, C., Bernhofer, C., Black, K. G., Bonal, D., Bonnefond, J. M., Chambers, J., Ciais, P., … Janssens, I. A. (2007). CO_2 balance of boreal, temperate, and tropical forests derived from a global database. *Global Change Biology*, 13(12), 2509–2537. https://doi.org/10.1111/j.1365-2486.2007.01439.x

Ma, H., Mo, L., Crowther, T. W., Maynard, D. S., van den Hoogen, J., Stocker, B. D., Terrer, C., & Zohner, C. M. (2021). The global distribution and environmental drivers of aboveground versus belowground plant biomass. *Nature Ecology & Evolution*, 5(8), 1110–1122. https://doi.org/10.1038/s41559-021-01485-1

Ma, S., He, F., Tian, D., Zou, D., Yan, Z., Yang, Y., Zhou, T., Huang, K., Shen, H., & Fang, J. (2018). Variations and determinants of carbon content in plants: A global synthesis. *Biogeosciences*, 15(3), 693–702. https://doi.org/10.5194/bg-15-693-2018

Maire, V., Wright, I. J., Prentice, I. C., Batjes, N. H., Bhaskar, R., van Bodegom, P. M., Cornwell, W. K., Ellsworth, D., Niinemets, Ü., Ordonez, A., Reich, P. B., & Santiago, L. S. (2015). Global effects of soil and climate on leaf photosynthetic traits and rates. *Global Ecology and Biogeography*, 24(6), 706–717. https://doi.org/10.1111/geb.12296

Malhi, Y., Doughty, C., & Galbraith, D. (2011). The allocation of ecosystem net primary productivity in tropical forests. *Philosophical Transactions of the Royal Society, B: Biological Sciences*, 366(1582), 3225–3245. https://doi.org/10.1098/rstb.2011.0062

Malhi, Y., Girardin, C. A. J., Goldsmith, G. R., Doughty, C. E., Salinas, N., Metcalfe, D. B., Huaraca Huasco, W., Silva-Espejo, J. E., del Aguilla-Pasquell, J., Farfán Amézquita, F., Aragão, L. E. O. C., Guerrieri, R., Ishida, F. Y., Bahar, N. H. A., Farfan-Rios, W., Phillips, O. L., Meir, P., & Silman, M. (2017). The variation of productivity and its allocation along a tropical elevation gradient: A whole carbon budget perspective. *New Phytologist*, 214(3), 1019–1032. https://doi.org/10.1111/nph.14189

Mauritsen, T., Bader, J., Becker, T., Behrens, J., Bittner, M., Brokopf, R., Brovkin, V., Claussen, M., Crueger, T., Esch, M., Fast, I., Fiedler, S., Fläschner, D., Gayler, V., Giorgetta, M., Goll, D. S., Haak, H., Hagemann, S., Hedemann, C., … Roeckner, E. (2019). Developments in the MPI-M earth system model version 1.2 (MPI-ESM1.2) and its response to increasing CO_2. *Journal of Advances in Modeling Earth Systems*, 11(4), 998–1038. https://doi.org/10.1029/2018MS001400

Medlyn, B. E., Zaehle, S., De Kauwe, M. G., Walker, A. P., Dietze, M. C., Hanson, P. J., Hickler, T., Jain, A. K., Luo, Y., Parton, W., Prentice, I. C., Thornton, P. E., Wang, S., Wang, Y. P., Weng, E., Iversen, C. M., Mccarthy, H. R., Warren, J. M., Oren, R., & Norby, R. J. (2015). Using ecosystem experiments to improve vegetation models. *Nature Climate Change*, 5(6), 528–534. https://doi.org/10.1038/nclimate2621

Meir, P., Levy, P. E., Grace, J., Jarvis, P. G., Ecology, S. P., Meir, P., Levy, P. E., Grace, J., & Jarvis, P. G. (2017). Photosynthetic parameters from two contrasting woody vegetation types in West Africa. *Plant Ecology*, 192(2), 277–287. https://doi.org/10.1007/s11258-007-9320-y

Meiyappan, P., Jain, A. K., & House, J. I. (2015). Increased influence of nitrogen limitation on CO_2 emissions from future land use and land use change. *Global Biogeochemical Cycles*, 29(9), 1524–1548. https://doi.org/10.1002/2015GB005086

Melillo, J. M., McGuire, A. D., Kicklighter, D. W., Moore, B., Vorosmarty, C. J., & Schloss, A. L. (1993). Global climate change and terrestrial net primary production. *Nature*, 363(6426), 234–240. https://doi.org/10.1038/363234a0

Melton, J. R., & Arora, V. K. (2016). Competition between plant functional types in the Canadian Terrestrial Ecosystem Model (CTEM)

v. 2.0. *Geoscientific Model Development*, 9(1), 323–361. https://doi.org/10.5194/gmd-9-323-2016

Mencuccini, M., & Grace, J. (1995). Climate influences the leaf area/sapwood area ratio in scots pine. *Tree Physiology*, 15(1), 1–10. https://doi.org/10.1093/treephys/15.1.1

Moreno-Martínez, Á., Camps-Valls, G., Kattge, J., Robinson, N., Reichstein, M., Bodegom, P. V., Kramer, K., Cornelissen, J. H. C., Reich, P. B., Bahn, M., Niinemets, Ü., Peñuelas, J., Craine, J., Cerabolini, B., Minden, V., Laughlin, D. C., Sack, L., & Allr, S. W. (2018). A methodology to derive global maps of leaf traits using remote sensing and climate data. *Remote Sensing of Environment*, 218, 69–88. https://doi.org/10.1016/j.rse.2018.09.006

Mori, S., Yamaji, K., Ishida, A., Prokushkin, S. G., Masyagina, O. V., Hagihara, A., Hoque, A. T. M. R., Suwa, R., Osawa, A., Nishizono, T., Ueda, T., Kinjo, M., Miyagi, T., Kajimoto, T., Koike, T., Matsuura, Y., Toma, T., Zyryanova, O. A., Abaimov, A. P., ... Umari, M. (2010). Mixed-power scaling of whole-plant respiration from seedlings to giant trees. *Proceedings of the National Academy of Sciences of the United States of America*, 107(4), 1447–1451. https://doi.org/10.1073/pnas.0902554107

Näsholm, T. (1998). Qualitative and quantitative changes in plant nitrogen acquisition induced by anthropogenic nitrogen deposition. *New Phytologist*, 139(1), 87–90. https://doi.org/10.1046/j.1469-8137.1998.00174.x

Näsholm, T., Kielland, K., & Ganeteg, U. (2009). Uptake of organic nitrogen by plants. *New Phytologist*, 182(1), 31–48. https://doi.org/10.1111/j.1469-8137.2008.02751.x

Norby, R. J., Warren, J. M., Iversen, C. M., Medlyn, B. E., & McMurtrie, R. E. (2010). CO_2 enhancement of forest productivity constrained by limited nitrogen availability. *Proceedings of the National Academy of Sciences of the United States of America*, 107(45), 19368–19373. https://doi.org/10.1073/pnas.1006463107

Oleson, K. W., Lawrence, D. M., Bonan, G. B., Drewniak, B., Huang, M., Koven, C. D., Levis, S., Li, F., Riley, W. J., Subin, Z. M., Swenson, S. C., Thornton, P. E., Bozbiyik, A., Fisher, R., Heald, C. L., Kluzek, E., Lamarque, J.-F., Lawrence, P. J., Leung, L. R., ... Yang, Z.-L. (2010). *Technical description of version 4.5 of the community land model (CLM)*. April, NCAR/TN-503+STR. http://www.cesm.ucar.edu/models/cesm1.2/clm/CLM45_Tech_Note.pdf

Peng, Y. (2023). yunkepeng/CNuptake_MS: CN uptake manuscript code and data (6.0). *Zenodo*, https://doi.org/10.5281/zenodo.8182205

Peng, Y., Bloomfield, K. J., Cernusak, L. A., Domingues, T. F., & Colin Prentice, I. (2021). Global climate and nutrient controls of photosynthetic capacity. *Communications Biology*, 4(1), 1–9. https://doi.org/10.1038/s42003-021-01985-7

Peng, Y., Guo, D., & Yang, Y. (2017). Global patterns of root dynamics under nitrogen enrichment. *Global Ecology and Biogeography*, 26(1), 102–114. https://doi.org/10.1111/geb.12508

Peñuelas, J., Fernández-Martínez, M., Ciais, P., Jou, D., Piao, S., Obersteiner, M., Vicca, S., Janssens, I. A., & Sardans, J. (2019). The bioelements, the elementome, and the biogeochemical niche. *Ecology*, 100(5), 1–15. https://doi.org/10.1002/ecy.2652

Penuelas, J., Fernández-Martínez, M., Vallicrosa, H., Maspons, J., Zuccarini, P., Carnicer, J., Sanders, T. G. M., Krüger, I., Obersteiner, M., Janssens, I. A., Ciais, P., & Sardans, J. (2020). Increasing atmospheric CO_2 concentrations correlate with declining nutritional status of European forests. *Communications Biology*, 3(1), 1–11. https://doi.org/10.1038/s42003-020-0839-y

Perkowski, E. A., Waring, E. F., & Smith, N. G. (2021). Root mass carbon costs to acquire nitrogen are determined by nitrogen and light availability in two species with different nitrogen acquisition strategies. *Journal of Experimental Botany*, 72(15), 5766–5776. https://doi.org/10.1093/jxb/erab253

Phillips, R. P., Brzostek, E., & Midgley, M. G. (2013). The mycorrhizal-associated nutrient economy: A new framework for predicting carbon-nutrient couplings in temperate forests. *New Phytologist*, 199(1), 41–51. https://doi.org/10.1111/nph.12221

Pinzon, J. E., & Tucker, C. J. (2014). A non-stationary 1981-2012 AVHRR NDVI3g time series. *Remote Sensing*, 6(8), 6929–6960. https://doi.org/10.3390/rs6086929

Poorter, H., Knopf, O., Wright, I. J., Temme, A., Hogewoning, S. W., Graf, A., Cernusak, L. A., & Pons, T. L. (2022). A meta-analysis of responses of C3 plants to atmospheric CO_2: Dose-response curves for 85 traits ranging from the molecular to the whole plant level. *New Phytologist*, 233(4), 1560–1596. https://doi.org/10.1111/nph.17802

Poorter, H., Niklas, K. J., Reich, P. B., Oleksyn, J., Poot, P., & Mommer, L. (2012). Biomass allocation to leaves, stems and roots: Meta-analyses of interspecific variation and environmental control. *New Phytologist*, 193(1), 30–50. https://doi.org/10.1111/j.1469-8137.2011.03952.x

Poulter, B., Aragão, L., Andela, N., Bellassen, V., Ciais, P., Kato, T., Lin, X., Nachin, B., Luyssaert, S., Pederson, N., Peylin, P., Piao, S., Saatchi, S., Schepaschenko, D., Schelhaas, M., & Shivdenko, A. (2018). *The global forest age dataset (GFADv1.0), link to NetCDF file*. NASA National Aeronautics and Space Administration, PANGAEA. https://doi.org/10.1594/PANGAEA.889943

Pregitzer, K. S., Burton, A. J., King, J. S., & Zak, D. R. (2008). Soil respiration, root biomass, and root turnover following long-term exposure of northern forests to elevated atmospheric CO_2 and tropospheric O_3. *New Phytologist*, 180(1), 153–161. https://doi.org/10.1111/j.1469-8137.2008.02564.x

Prentice, I. C., Dong, N., Gleason, S. M., Maire, V., & Wright, I. J. (2014). Balancing the costs of carbon gain and water transport: Testing a new theoretical framework for plant functional ecology. *Ecology Letters*, 17(1), 82–91. https://doi.org/10.1111/ele.12211

Radujković, D., Verbruggen, E., Seabloom, E. W., Bahn, M., Biederman, L. A., Borer, E. T., Boughton, E. H., Catford, J. A., Campioli, M., Donohue, I., Ebeling, A., Eskelinen, A., Fay, P. A., Hansart, A., Knops, J. M. H., MacDougall, A. S., Ohlert, T., Olde Venterink, H., Raynaud, X., ... Vicca, S. (2021). Soil properties as key predictors of global grassland production: Have we overlooked micronutrients? *Ecology Letters*, 24(12), 2713–2725. https://doi.org/10.1111/ele.13894

Reay, D. S., Dentener, F., Smith, P., Grace, J., & Feely, R. A. (2008). Global nitrogen deposition and carbon sinks. *Nature Geoscience*, 1(7), 430–437. https://doi.org/10.1038/ngeo230

Reich, P. B., Tjoelker, M. G., Pregitzer, K. S., Wright, I. J., Oleksyn, J., & Machado, J. L. (2008). Scaling of respiration to nitrogen in leaves, stems and roots of higher land plants. *Ecology Letters*, 11(8), 793–801. https://doi.org/10.1111/j.1461-0248.2008.01185.x

Reich, P. B., Wright, I. J., & Lusk, C. H. (2007). Predicting leaf physiology from simple plant and climate attributes: A global glopnet analysis. *Ecological Applications*, 17(7), 1982–1988. https://doi.org/10.1890/06-1803.1

Ryan, M. G., Binkley, D., Fownes, J. H., Giardina, C. P., & Senock, R. S. (2004). An experimental test of the causes of forest growth decline with stand age. *Ecological Monographs*, 74(3), 393–414. https://doi.org/10.1890/03-4037

Sardans, J., Vallicrosa, H., Zuccarini, P., Farré-Armengol, G., Fernández-Martínez, M., Peguero, G., Gargallo-Garriga, A., Ciais, P., Janssens, I. A., Obersteiner, M., Richter, A., & Peñuelas, J. (2021). Empirical support for the biogeochemical niche hypothesis in forest trees. *Nature Ecology & Evolution*, 5(2), 184–194. https://doi.org/10.1038/s41559-020-01348-1

Schenk, H. J., & Jackson, R. B. (2002). Rooting depths, lateral root spreads and below-ground/above-ground allometries of plants in water-limited ecosystems. *Journal of Ecology*, 90(3), 480–494. https://doi.org/10.1046/j.1365-2745.2002.00682.x

Schreeg, L. A., Santiago, L. S., Wright, S. J., & Turner, B. L. (2014). Stem, root, and older leaf N:P ratios are more responsive indicators of soil nutrient availability than new foliage. *Ecology*, 95(8), 2062–2068. https://doi.org/10.1890/13-1671.1

Sellar, A. A., Jones, C. G., Mulcahy, J. P., Tang, Y., Yool, A., Wiltshire, A., O'Connor, F. M., Stringer, M., Hill, R., Palmieri, J., Woodward, S., de Mora, L., Kuhlbrodt, T., Rumbold, S. T., Kelley, D. I., Ellis, R., Johnson,

C. E., Walton, J., Abraham, N. L., … Zerroukat, M. (2019). UKESM1: Description and evaluation of the U.K. earth system model. *Journal of Advances in Modeling Earth Systems*, 11(12), 4513–4558. https://doi.org/10.1029/2019MS001739

Smith, B., Wärlind, D., Arneth, A., Hickler, T., Leadley, P., Siltberg, J., & Zaehle, S. (2014). Implications of incorporating N cycling and N limitations on primary production in an individual-based dynamic vegetation model. *Biogeosciences*, 11(7), 2027–2054. https://doi.org/10.5194/bg-11-2027-2014

Smith, N. G., Keenan, T. F., Colin Prentice, I., Wang, H., Wright, I. J., Niinemets, Ü., Crous, K. Y., Domingues, T. F., Guerrieri, R., Yoko Ishida, F., Kattge, J., Kruger, E. L., Maire, V., Rogers, A., Serbin, S. P., Tarvainen, L., Togashi, H. F., Townsend, P. A., Wang, M., … Zhou, S. X. (2019). Global photosynthetic capacity is optimized to the environment. *Ecology Letters*, 22(3), 506–517. https://doi.org/10.1111/ele.13210

Stocker, B. D., Prentice, I. C., Cornell, S. E., Davies-Barnard, T., Finzi, A. C., Franklin, O., Janssens, I., Larmola, T., Manzoni, S., Näsholm, T., Raven, J. A., Rebel, K. T., Reed, S., Vicca, S., Wiltshire, A., & Zaehle, S. (2016). Terrestrial nitrogen cycling in earth system models revisited. *New Phytologist*, 210(4), 1165–1168. https://doi.org/10.1111/nph.13997

Stocker, B. D., Wang, H., Smith, N. G., Harrison, S. P., Keenan, T. F., Sandoval, D., Davis, T., & Prentice, I. C. (2020). P-model v1.0: An optimality-based light use efficiency model for simulating ecosystem gross primary production. *Geoscientific Model Development*, 13(3), 1545–1581. https://doi.org/10.5194/gmd-13-1545-2020

Sulla-Menashe, D., & Friedl, M. A. (2018). *User guide to collection 6 MODIS land cover (MCD12Q1 and MCD12C1) product*. USGS. https://lpdaac.usgs.gov/documents/101/MCD12_User_Guide_V6.pdf

Tang, X., Zhao, X., Bai, Y., Tang, Z., Wang, W., Zhao, Y., Wan, H., Xie, Z., Shi, X., Wu, B., Wang, G., Yan, J., Ma, K., Du, S., Li, S., Han, S., Ma, Y., Hu, H., He, N., … Zhou, G. (2018). Carbon pools in China's terrestrial ecosystems: New estimates based on an intensive field survey. *Proceedings of the National Academy of Sciences of the United States of America*, 115(16), 4021–4026. https://doi.org/10.1073/pnas.1700291115

Terrer, C., Jackson, R. B., Prentice, I. C., Keenan, T. F., Kaiser, C., Vicca, S., Fisher, J. B., Reich, P. B., Stocker, B. D., Hungate, B. A., Peñuelas, J., McCallum, I., Soudzilovskaia, N. A., Cernusak, L. A., Talhelm, A. F., Van Sundert, K., Piao, S., Newton, P. C. D., Hovenden, M. J., … Franklin, O. (2019). Nitrogen and phosphorus constrain the CO_2 fertilization of global plant biomass. *Nature Climate Change*, 9(9), 684–689. https://doi.org/10.1038/s41558-019-0545-2

Terrer, C., Vicca, S., Stocker, B. D., Hungate, B. A., Phillips, R. P., Reich, P. B., Finzi, A. C., & Prentice, I. C. (2018). Ecosystem responses to elevated CO_2 governed by plant–soil interactions and the cost of nitrogen acquisition. *New Phytologist*, 217(2), 507–522. https://doi.org/10.1111/nph.14872

Tian, D., Kattge, J., Chen, Y., Han, W., Luo, Y., He, J., Hu, H., Tang, Z., Ma, S., Yan, Z., Lin, Q., Schmid, B., & Fang, J. (2019). A global database of paired leaf nitrogen and phosphorus concentrations of terrestrial plants. *Ecology*, 100(9), 2812. https://doi.org/10.1002/ecy.2812

Van Sundert, K., Radujković, D., Cools, N., De Vos, B., Etzold, S., Fernández-Martínez, M., Janssens, I. A., Merilä, P., Peñuelas, J., Sardans, J., Stendahl, J., Terrer, C., & Vicca, S. (2020). Towards comparable assessment of the soil nutrient status across scales—Review and development of nutrient metrics. *Global Change Biology*, 26(2), 392–409. https://doi.org/10.1111/gcb.14802

Ven, A., Verlinden, M. S., Fransen, E., Olsson, P. A., Verbruggen, E., Wallander, H., & Vicca, S. (2020). Phosphorus addition increased carbon partitioning to autotrophic respiration but not to biomass production in an experiment with Zea mays. *Plant, Cell and Environment*, 43(9), 2054–2065. https://doi.org/10.1111/pce.13785

Ven, A., Verlinden, M. S., Verbruggen, E., & Vicca, S. (2019). Experimental evidence that phosphorus fertilization and arbuscular mycorrhizal symbiosis can reduce the carbon cost of phosphorus uptake. *Functional Ecology*, 33(11), 2215–2225. https://doi.org/10.1111/1365-2435.13452

Vicca, S., Luyssaert, S., Peñuelas, J., Campioli, M., Chapin, F. S., Ciais, P., Heinemeyer, A., Högberg, P., Kutsch, W. L., Law, B. E., Malhi, Y., Papale, D., Piao, S. L., Reichstein, M., Schulze, E. D., & Janssens, I. A. (2012). Fertile forests produce biomass more efficiently. *Ecology Letters*, 15(6), 520–526. https://doi.org/10.1111/j.1461-0248.2012.01775.x

Vicca, S., Stocker, B. D., Reed, S., Wieder, W. R., Bahn, M., Fay, P. A., Janssens, I. A., Lambers, H., Peñuelas, J., Piao, S., Rebel, K. T., Sardans, J., Sigurdsson, B. D., Van Sundert, K., Wang, Y. P., Zaehle, S., & Ciais, P. (2018). Using research networks to create the comprehensive datasets needed to assess nutrient availability as a key determinant of terrestrial carbon cycling. *Environmental Research Letters*, 13(12), 125006. https://doi.org/10.1088/1748-9326/aaeae7

Walker, A. P., Aranda, I., Beckerman, A. P., Bown, H., Cernusak, L. A., Dang, Q. L., Domingues, T. F., Gu, L., Guo, S., Han, Q., Kattge, J., Kubiske, M., Manter, D., Merilo, E., Midgley, G. F., Porte, A., Scales, J. C., Tissue, D., Turnbull, T., … Wullschleger, S. D. (2014). *A global data set of leaf photosynthetic rates, leaf N and P, and specific leaf area*. ORNL DAAC. https://doi.org/10.3334/ORNLDAAC/1224

Walker, A. P., Quaife, T., van Bodegom, P. M., De Kauwe, M. G., Keenan, T. F., Joiner, J., Lomas, M. R., MacBean, N., Xu, C., Yang, X., & Woodward, F. I. (2017). The impact of alternative trait-scaling hypotheses for the maximum photosynthetic carboxylation rate (V_{cmax}) on global gross primary production. *New Phytologist*, 215(4), 1370–1386. https://doi.org/10.1111/nph.14623

Wang, H., Harrison, S. P., Prentice, I. C., Yang, Y., Bai, F., Togashi, H. F., Wang, M., Zhou, S., & Ni, J. (2018). The China plant trait database: Toward a comprehensive regional compilation of functional traits for land plants. *Ecology*, 99(2), 500. https://doi.org/10.1002/ecy.2091

Wang, H., Prentice, I. C., Keenan, T. F., Davis, T. W., Wright, I. J., Cornwell, W. K., Evans, B. J., & Peng, C. (2017). Towards a universal model for carbon dioxide uptake by plants. *Nature Plants*, 3(9), 734–741. https://doi.org/10.1038/s41477-017-0006-8

Wang, H., Prentice, I. C., Wright, I. J., Warton, D. I., Qiao, S., Xu, X., Zhou, J., Kikuzawa, K., & Stenseth, N. C. (2023). Leaf economics fundamentals explained by optimality principles. *Science. Advances*, 9(3), eadd5667. https://doi.org/10.1126/sciadv.add5667

Wang, X., & Zhao, X. (Eds.). (2022). *Protocol for field investigation and literature data compilation of carbon storage in terrestrial ecosystems*. Science Press.

Wang, Y., Ciais, P., Goll, D., Huang, Y., Luo, Y., Wang, Y. P., Bloom, A. A., Broquet, G., Hartmann, J., Peng, S., Penuelas, J., Piao, S., Sardans, J., Stocker, B. D., Wang, R., Zaehle, S., & Zechmeister-Boltenstern, S. (2018). GOLUM-CNP v1.0: A data-driven modeling of carbon, nitrogen and phosphorus cycles in major terrestrial biomes. *Geoscientific Model Development*, 11(9), 3903–3928. https://doi.org/10.5194/gmd-11-3903-2018

Weedon, G. P., Balsamo, G., Bellouin, N., Gomes, S., Best, M. J., & Viterbo, P. (2014). Data methodology applied to ERA-interim reanalysis data. *Water Resources Research*, 50(9), 7505–7514. https://doi.org/10.1002/2014WR015638

Wiltshire, A. J., Burke, E. J., Chadburn, S. E., Jones, C. D., Cox, P. M., Davies-Barnard, T., Friedlingstein, P., Harper, A. B., Liddicoat, S., Sitch, S., & Zaehle, S. (2021). JULES-CN: A coupled terrestrial carbon-nitrogen scheme (JULES vn5.1). *Geoscientific Model Development*, 14(4), 2161–2186. https://doi.org/10.5194/gmd-14-2161-2021

Xia, J., Yuan, W., Lienert, S., Joos, F., Ciais, P., Viovy, N., Wang, Y. P., Wang, X., Zhang, H., Chen, Y., & Tian, X. (2019). Global patterns in net primary production allocation regulated by environmental conditions and Forest stand age: A model-data comparison. *Journal of Geophysical Research: Biogeosciences*, 124(7), 2039–2059. https://doi.org/10.1029/2018JG004777

Xu, H., Wang, H., Prentice, I. C., Harrison, S. P., Wang, G., & Sun, X. (2021). Predictability of leaf traits with climate and elevation: A case study in

Gongga Mountain, China. *Tree Physiology*, 41(8), 1336–1352. https://doi.org/10.1093/treephys/tpab003

Yan, Z., Eziz, A., Tian, D., Li, X., Hou, X., Peng, H., Han, W., Guo, Y., & Fang, J. (2019). Biomass allocation in response to nitrogen and phosphorus availability: Insight from experimental manipulations of *Arabidopsis thaliana*. *Frontiers in Plant Science*, 10, 598. https://doi.org/10.3389/fpls.2019.00598

Zaehle, S., Friend, A. D., Friedlingstein, P., Dentener, F., Peylin, P., & Schulz, M. (2010). Carbon and nitrogen cycle dynamics in the O-CN land surface model: 2. Role of the nitrogen cycle in the historical terrestrial carbon balance. *Global Biogeochemical Cycles*, 24(1). https://doi.org/10.1029/2009gb003522

Zaehle, S., Medlyn, B. E., De Kauwe, M. G., Walker, A. P., Dietze, M. C., Hickler, T., Luo, Y., Wang, Y. P., El-Masri, B., Thornton, P., Jain, A., Wang, S., Warlind, D., Weng, E., Parton, W., Iversen, C. M., Gallet-Budynek, A., Mccarthy, H., Finzi, A., ... Norby, R. J. (2014). Evaluation of 11 terrestrial carbon-nitrogen cycle models against observations from two temperate free-air CO_2 enrichment studies. *New Phytologist*, 202(3), 803–822. https://doi.org/10.1111/nph.12697

Zak, D. R., Pregitzer, K. S., Kubiske, M. E., & Burton, A. J. (2011). Forest productivity under elevated CO_2 and O_3: Positive feedbacks to soil N cycling sustain decade-long net primary productivity enhancement by CO_2. *Ecology Letters*, 14(12), 1220–1226. https://doi.org/10.1111/j.1461-0248.2011.01692.x

Zhang, B., Cadotte, M. W., Chen, S., Tan, X., You, C., Ren, T., Chen, M., Wang, S., Li, W., Chu, C., Jiang, L., Bai, Y., Huang, J., & Han, X. (2019). Plants alter their vertical root distribution rather than biomass allocation in response to changing precipitation. *Ecology*, 100(11), e02828. https://doi.org/10.1002/ecy.2828

Zhang, J., He, N., Liu, C., Xu, L., Chen, Z., Li, Y., Wang, R., Yu, G., Sun, W., Xiao, C., Chen, H. Y. H., & Reich, P. B. (2020). Variation and evolution of C:N ratio among different organs enable plants to adapt to N-limited environments. *Global Change Biology*, 26(4), 2534–2543. https://doi.org/10.1111/gcb.14973

Zhao, M., & Running, S. W. (2010). Drought-induced reduction in global terrestrial net primary production from 2000 through 2009. *Science*, 329(5994), 940–943. https://doi.org/10.1126/science.1192666

SUPPORTING INFORMATION

Additional supporting information can be found online in the Supporting Information section at the end of this article.

Table S1: Reference information of biomass production dataset in grassland.

Table S2: Model selection for stepwise forward regression.

Table S3: Simulated global C and N uptakes. Units are $Pg\,C\,year^{-1}$ or $Pg\,N\,year^{-1}$.

Figure S1: Flowchart for data-driven model estimation and global simulation of carbon and nitrogen cycling. In forests and grasslands, empirical models and constants were designed to determine biomass production (BP; $g\,C\,m^{-2}\,year^{-1}$); the ratio of aboveground biomass production (ABP; $g\,C\,m^{-2}\,year^{-1}$) to BP; the ratio of leaf biomass production (BPleaf; $g\,C\,m^{-2}\,year^{-1}$) to ABP; leaf nitrogen per mass (N_{mass}; unitless); wood and root carbon-to-nitrogen ratio (C:N; $g\,C/g\,N$) and nitrogen resorption efficiency (NRE; unitless).

Figure S2: Global simulations of biomass production (BP; $g\,C\,m^{-2}\,year^{-1}$), above-ground biomass production (ABP; $g\,C\,m^{-2}\,year^{-1}$), leaf carbon-to-nitrogen ratio (leaf C/N), nitrogen resorption efficiency (NRE), terrestrial N uptake ($g\,N\,m^{-2}\,year^{-1}$) and nitrogen-use-efficiency (NUE).

Figure S3: Multicollinearity VIF analysis for fitted BP, ABP/BP, and leaf-BP/ABP models.

Figure S4: All prediction fields mapped for site and global simulations: soil carbon to nitrogen ratio (C/N) (Batjes, 2015), stand-age (age) (Poulter et al., 2018), fraction of absorbed photosynthetically active radiation (fAPAR) (Pinzon & Tucker, 2014), incident photosynthetic photon flux density averaged over the growing season (gPPFD) (Weedon et al., 2014), growth temperature (T_g) (Harris et al., 2014), vapour pressure deficit (D) (Harris et al., 2014), maximum rate of carboxylation at 25°C (V_{cmax25}) (Stocker et al., 2020) and leaf mass-per-area (LMA) (Moreno-Martinez et al. 2018).

Figure S5: Partial residual plots for statistical models developed to predict: (1) biomass production (BP; $g\,C\,m^{-2}\,year^{-1}$) in forest; (2) the ratio of aboveground biomass production (ABP; $g\,C\,m^{-2}\,year^{-1}$) to BP.

Figure S6: Bi-variate relationship between nitrogen-use-efficiency (NUE) and leaf-BP/ABP basing on global prediction from data-driven model.